The Plant Cell, Vol. 17, 1233–1251, April 2005, www.plantcell.org

Two P-Type ATPases Are Required for Copper Delivery in *Arabidopsis thaliana* Chloroplasts

Salah E. Abdel-Ghany,[a] Patricia Müller-Moulé,[b,1] Krishna K. Niyogi,[b] Marinus Pilon,[a,2] and Toshiharu Shikanai[c]

[a] Biology Department, Colorado State University, Fort Collins, Colorado 80523
[b] Department of Plant and Microbial Biology, University of California, Berkeley, California 94720-3102
[c] Graduate School of Agriculture, Kyushu University, Fukuoka 812-8581, Japan

Copper delivery to the thylakoid lumen protein plastocyanin and the stromal enzyme Cu/Zn superoxide dismutase in chloroplasts is required for photosynthesis and oxidative stress protection. The copper delivery system in chloroplasts was characterized by analyzing the function of copper transporter genes in *Arabidopsis thaliana*. Two mutant alleles were identified of a previously uncharacterized gene, *PAA2* (for P-type ATPase of Arabidopsis), which is required for efficient photosynthetic electron transport. *PAA2* encodes a copper-transporting P-type ATPase with sequence similarity to PAA1, which functions in copper transport in chloroplasts. Both proteins localized to the chloroplast, as indicated by fusions to green fluorescent protein. The PAA1 fusions were found in the chloroplast periphery, whereas PAA2 fusions were localized in thylakoid membranes. The phenotypes of *paa1* and *paa2* mutants indicated that the two transporters have distinct functions: whereas both transporters are required for copper delivery to plastocyanin, copper delivery to the stroma is inhibited only in *paa1* but not in *paa2*. The effects of *paa1* and *paa2* on superoxide dismutase isoform expression levels suggest that stromal copper levels regulate expression of the nuclear genes *IRON SUPEROXIDE DISMUTASE1* and *COPPER/ZINC SUPEROXIDE DISMUTASE2*. A *paa1 paa2* double mutant was seedling-lethal, underscoring the importance of copper to photosynthesis. We propose that PAA1 and PAA2 function sequentially in copper transport over the envelope and thylakoid membrane, respectively.

INTRODUCTION

For plant survival and productivity, mineral nutrients have to be delivered in adequate amounts to the various subcellular compartments. Despite the importance of intracellular mineral transport and homeostasis, there is still much to be learned about the mechanisms involved. The goal of this study was to obtain insight into the mechanisms involved in the transport and homeostasis of Cu in chloroplasts. Homeostasis of this element must be tightly controlled because Cu is both an essential nutrient for electron transport processes and also very toxic when present in excess. The chloroplast is an ideal model organelle in which to study Cu homeostasis because it is a major sink for Cu in plants (Marschner, 1995). Furthermore, photosynthetic electron transport can be assessed directly in intact plants, and the activity of plastid Cu proteins can be assayed in isolated organelles (Shikanai et al., 2003).

In chloroplasts, Cu is an important cofactor for photosynthetic electron transport (Raven et al., 1999). Plastocyanin, a blue Cu protein, catalyzes electron transfer between the cytochrome b_6f complex and photosystem I (PSI) in the thylakoid lumen of oxygenic photosynthetic organisms (Raven et al., 1999). Plastocyanin is one of the most abundant proteins in the thylakoid lumen. *Arabidopsis thaliana* expresses two plastocyanin genes, which encode proteins that are closely related in sequence (Schubert et al., 2002).

Cu, together with Zn, also is a cofactor of Cu/ZnSOD (Bowler et al., 1994). In Arabidopsis, seven genes for superoxide dismutase (SOD) have been identified (Kliebenstein et al., 1998). The major SOD activities that are detectable in Arabidopsis are attributable to four genes: *COPPER/ZINC SUPEROXIDE DISMUTASE1* (*CSD1*), *CSD2*, *IRON SUPEROXIDE DISMUTASE1* (*FSD1*), and *MANGANESE SUPEROXIDE DISMUTASE1* (*MSD1*) (Kliebenstein et al., 1998). *CSD1* encodes a Cu/ZnSOD active in the cytosol, and *CSD2* encodes a Cu/ZnSOD active in the chloroplast stroma. *FSD1* encodes a SOD with an iron cofactor, FeSOD, which is also active in chloroplasts. The stromal SOD proteins are important to photosynthesis because of their role in the scavenging of reactive oxygen species in the water–water cycle (Asada, 1999). Finally, a MnSOD encoded by *MSD1* is active in mitochondria (Kliebenstein et al., 1998).

Despite its physiological importance to plants, Cu concentrations as low as 20 μM in agar media cause visible toxicity to Arabidopsis (Murphy and Taiz, 1995). To allow sufficient metal cofactor delivery to target proteins but at the same time avoid metal ion–induced damage, organisms may have evolved

[1] Current address: Institute for Developmental and Molecular Plant Biology, Building 26.03, University of Düsseldorf, 40225 Düsseldorf, Germany.
[2] To whom correspondence should be addressed. E-mail pilon@lamar.colostate.edu; fax 970-491-0649.
The author responsible for distribution of materials integral to the findings presented in this article in accordance with the policy described in the Instructions for Authors (www.plantcell.org) is: Marinus Pilon (pilon@lamar.colostate.edu).
Article, publication date, and citation information can be found at www.plantcell.org/cgi/doi/10.1105/tpc.104.030452.

delivery systems composed of specific membrane transporters and soluble binding proteins that together avoid the accumulation of free metal ions in cells (Nelson, 1999). In Arabidopsis, the *COPT1* gene and its four homologs encode Cu transporters that may allow the entrance of Cu into plant cells (Kampfenkel et al., 1995; Sancenon et al., 2003). With respect to intracellular Cu transport and homeostasis, several plant homologs of Cu trafficking proteins that function in animals and in fungi, particularly yeast, have been discovered (for reviews, see Fox and Guerinot, 1998; Himelblau and Amasino, 2000; Williams et al., 2000). The components identified include the metallothioneins *MT2a* and *MT3* (Guo et al., 2003) as well as *CCH1* (Himelblau et al., 1998), which encodes a functional homolog of the yeast Cu chaperone *ATX1* (Lin et al., 1997; Pufahl et al., 1997). The Arabidopsis gene *RAN1* is required for Cu delivery to the ethylene receptors (Hirayama et al., 1999) and is a homolog of the genes that encode Cu-transporting P-type ATPases that are functional in the endomembrane system of *Chlamydomonas reinhardtii* (La Fontaine et al., 2002) and yeast (Askwith et al., 1994; Dancis et al., 1994; Yuan et al., 1995).

Chloroplasts have a complex internal structure, and Cu must be delivered in a regulated manner to very defined locations within the organelle. In Synechocystis, a cyanobacterium that shares evolutionary ancestry with chloroplasts, two Cu-transporting P-type ATPases have been characterized. CtaA functions in Cu import into the cell (Phung et al., 1994), whereas PacS is involved in thylakoid import (Kanamaru et al., 1994). Each of these proteins is required for efficient switching to the use of Cu in plastocyanin rather than heme Fe in cytochrome c_6 for photosynthetic electron transport (Tottey et al., 2001). A Cu chaperone, designated bacterial Atx1, has been discovered in a bacterial two-hybrid assay (Tottey et al., 2002). Bacterial Atx1 interacts with the N-terminal domains of both CtaA and PacS. Atx1 acquires Cu from CtaA or other sources in the cyanobacterial cytosol and donates Cu to PacS (Tottey et al., 2002). The first described component of the Cu delivery system to chloroplasts in plants is *PAA1* (for P-type ATPase of Arabidopsis), a member of the metal-transporting P-type ATPase family (Tabata et al., 1997; Shikanai et al., 2003). Here, we report the identification and functional characterization of a second Cu-transporting P-type ATPase, PAA2, which is active in chloroplasts and required for Cu delivery to the thylakoid lumen.

RESULTS

High Chlorophyll Fluorescence Mutants That Mapped to a Gene Encoding a Novel Cu-Transporting P-Type ATPase

Plants with even subtle defects in photosynthetic electron transport may display a high chlorophyll fluorescence phenotype, which can be detected using an imaging system (Niyogi et al., 1998; Shikanai et al., 1999, 2003). To obtain novel mutants with a defect in photosynthesis, $\sim 2 \times 10^4$ seedlings derived by mutagenesis with ethyl methanesulfonate were screened for a high fluorescence phenotype at a light intensity of 300 μmol·m^{-2}·s^{-1}. Among the Arabidopsis mutants isolated were two novel mutants, later designated *paa2-1* and *paa2-2* (see below). Except for the high chlorophyll fluorescence, *paa2* mutants did not exhibit any visible phenotype on regular soil (Figure 1). Genetic analysis revealed that the phenotype of both mutants was attributable to a recessive mutation in a single nuclear gene. F1 plants resulting from a cross between the two mutants displayed the high chlorophyll fluorescence, indicating that the two mutants were allelic.

To identify the gene responsible for the high chlorophyll fluorescence phenotype, *paa2-2* (Columbia [Col] background) was crossed to a polymorphic wild-type strain (Landsberg *erecta*), and the mutation was mapped between molecular markers T10F18 and MWD9 on chromosome 5 (Figure 2). Fine mapping using 337 F2 plants identified a 140-kb region covered by two BAC clones, T10F18 and T6G21. Because we expected the chlorophyll fluorescence phenotype to be associated with a chloroplast function, the genomic sequences of candidate genes encoding putative chloroplast-targeted proteins within the 140-kb region were determined and compared between mutants and wild-type plants. Sequence alterations were found in a single gene with the Arabidopsis Genome Initiative number At5g21930 in both alleles. To verify that At5g21930 is responsible for the mutant phenotype, the genomic sequence containing a single gene, the wild-type At5g21930, was introduced into *paa2-2*. The transformation complemented the chlorophyll fluorescence phenotype (Figure 1, *paa2-2* + *PAA2*). We conclude that the high fluorescence phenotype was attributable to lesions in At5g21930.

At5g21930 encodes a putative metal-transporting P-type ATPase (Solioz and Vulpe, 1996) and is most similar to *PAA1*, which encodes a Cu-transporting P-type ATPase in chloroplasts (Tabata et al., 1997; Shikanai et al., 2003). Therefore, we designated At5g21930 as *PAA2* and the two mutant alleles as *paa2-1* and *paa2-2*. A nonsense mutation was found in the second exon in *paa2-1*, suggesting that *paa2-1* is effectively a null allele. The mutation in *paa2-2* is a nucleotide substitution at the predicted junction between the second intron and the third

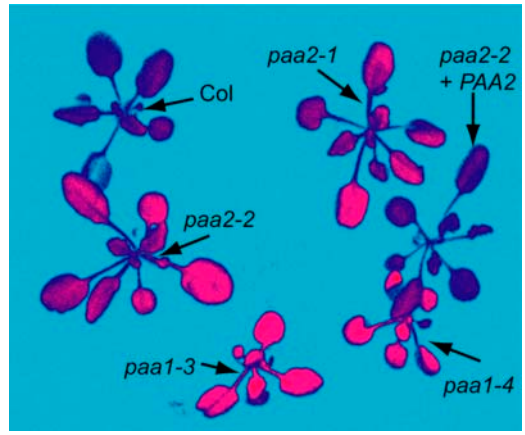

Figure 1. High Chlorophyll Fluorescence Phenotype of *paa2* Mutants.

Wild-type, *paa1*, and *paa2* seedlings were grown in soil for 4 weeks. A chlorophyll fluorescence image was captured after 1 min of illumination with actinic light (300 μmol·m^{-2}·s^{-1}). The fluorescence level is indicated by false coloring in this order: red > pink > blue. Col, Columbia *gl1* wild type; *paa2-2* + *PAA2*, *paa2-2* transformed with the genomic *PAA2* sequence.

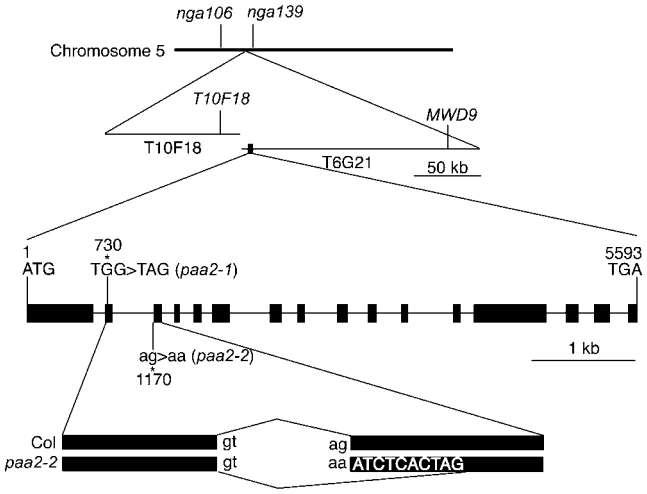

Figure 2. Positional Cloning of the *PAA2* Gene Encoding a Cu-Transporting P-Type ATPase.

The *paa2* mutation was mapped to the 140-kb region spanning two BAC clones (T10F18 and T6G21) on chromosome 5. The small box on T6G21 represents the position of *PAA2*. Exons (boxes) and introns (lines) were predicted from the cDNA sequence. The positions of the *paa2* mutations are indicated. The *paa2-2* mutation causes incorrect splicing of exons 2 and 3.

exon from the consensus AG (Brown et al., 1996) into AA. Sequencing of RT-PCR products revealed that a downstream AG in the third exon was used for splicing in the transcripts detected in *paa2-2*. The resulting frame shift should cause the premature termination of translation. Thus, based on sequence analysis, it is predicted that both *paa2-1* and *paa2-2* are null alleles. However, we cannot exclude the possibility that *paa2-2* may be leaky, because an alternative splicing mechanism in *paa2* may produce a minor, so far undetected, form of mRNA that could be translated into an at least partially functional protein.

A cDNA for the *PAA2* coding sequence was obtained by RT-PCR, and sequence analysis clarified that the exons of At5g21930/*PAA2* were incorrectly assigned in the Munich Information Center for Protein Sequences (http://mips.gsf.de/proj/thal/db/) and The Arabidopsis Information Resource (http://www.Arabidopsis.org/) databases. The first two predicted exons were not interrupted by an intron in the cDNA sequence. Thus, *PAA2* consists of 16 exons and 15 introns (Figure 2). The amino acid sequence of PAA2 with a correctly assigned exon 1 shows 43% amino acid identity with the PAA1 sequence (Figure 3A).

Like *PAA1*, *PAA2* is predicted to encode a precursor protein with a cleavable N-terminal chloroplast transit sequence (Figure 3A). Analysis of the predicted sequence of *PAA2* suggests that it encodes an integral membrane protein with eight possible transmembrane regions (Figure 3) and that has all of the characteristic conserved domains of the Cu-transporting P-type ATPases found in various organisms (Solioz and Vulpe, 1996; Axelsen and Palmgren, 2001). The conserved domains include a MxCxxC consensus metal binding motif in the N-terminal region, a CPC ion transduction domain in the sixth predicted transmembrane domain, a phosphorylation domain and an ATP binding domain in a large soluble domain loop between transmembrane domains 6 and 7, and a phosphatase domain in a smaller loop (Figure 3). Relative to PAA1, PAA2 lacks a Gly-rich region that follows the transit sequence cleavage site, and the hydrophobicity of the first two transmembrane regions of PAA2 is reduced.

paa2 Mutants Are Defective in Photosynthetic Electron Transport

The high chlorophyll fluorescence of *paa2* suggests that photosynthetic electron transport was affected, as was the case for *paa1* (Shikanai et al., 2003). Quantitative analysis of chlorophyll fluorescence enables us to monitor the status of photosynthetic electron transport in vivo (Krause and Weis, 1991). To determine quantitatively whether there are defects in photosynthetic electron transport, we measured the relative rate of photosystem II (PSII) electron transport as a function of light intensity. Figure 4 shows that the electron transport was affected in the *paa2* alleles even at relatively low light intensities (50 to 120 $\mu mol \cdot m^{-2} \cdot s^{-1}$) and that it was saturated at ~50% of the maximum electron transport in the wild type. Introduction of the wild-type *PAA2* sequence into *paa2-1* complemented the electron transport phenotype (Figure 4, *paa2-1* + *PAA2*). For comparison, we measured the electron transport in a *paa1* mutant in the same Col background. In *paa1-3*, electron transport was saturated at lower light intensity and reached a much lower level (~30% of the wild-type level) than in *paa2* mutants. We conclude that electron transport is impaired in *paa2*, although the effect is rather mild compared with that in *paa1*. This observation is consistent with the difference in growth rates on soil between *paa1* and *paa2* as estimated from seedling size (Figure 1).

The *PAA2* Phenotype Depends on Cu Availability

PAA2 has sequence similarity to genes encoding Cu-transporting P-type ATPases, and mutations in *PAA2* affect photosynthetic electron transport (Figure 4). To investigate whether the observed phenomena result from defects in Cu delivery, we tested the effects of Cu feeding on the phenotype of *paa2*. Two alleles of *paa2* and, for comparison, one allele of *paa1* and the wild type were cultured on solid agar medium with varying concentrations of $CuSO_4$ (Figure 5). Photosynthetic electron transport activity was estimated from the chlorophyll fluorescence parameter Φ_{PSII} (the efficiency of PSII photochemistry). Chlorophyll content was also determined because it is a good indicator of sensitivity to Cu (Shikanai et al., 2003).

Consistent with the reduction of electron transport in the seedlings cultured on soil (Figure 4), Φ_{PSII} was affected in both alleles of *paa2* on standard MS medium containing 0.1 μM $CuSO_4$. The phenotype of *paa2-1* was more severe than that of *paa2-2*, particularly on medium with very low Cu. As mentioned above, leakiness is a possibility in *paa2-2*, and this may explain the difference between the mutant alleles of *paa2*. Again, there was a stronger reduction in Φ_{PSII} in the *paa1* mutant. Addition of $CuSO_4$ (1 to 10 μM) restored Φ_{PSII} and chlorophyll content in *paa1-4*, as reported previously (Shikanai et al., 2003). The *paa2* phenotypes were also suppressed by growth on 1 or 10 μM

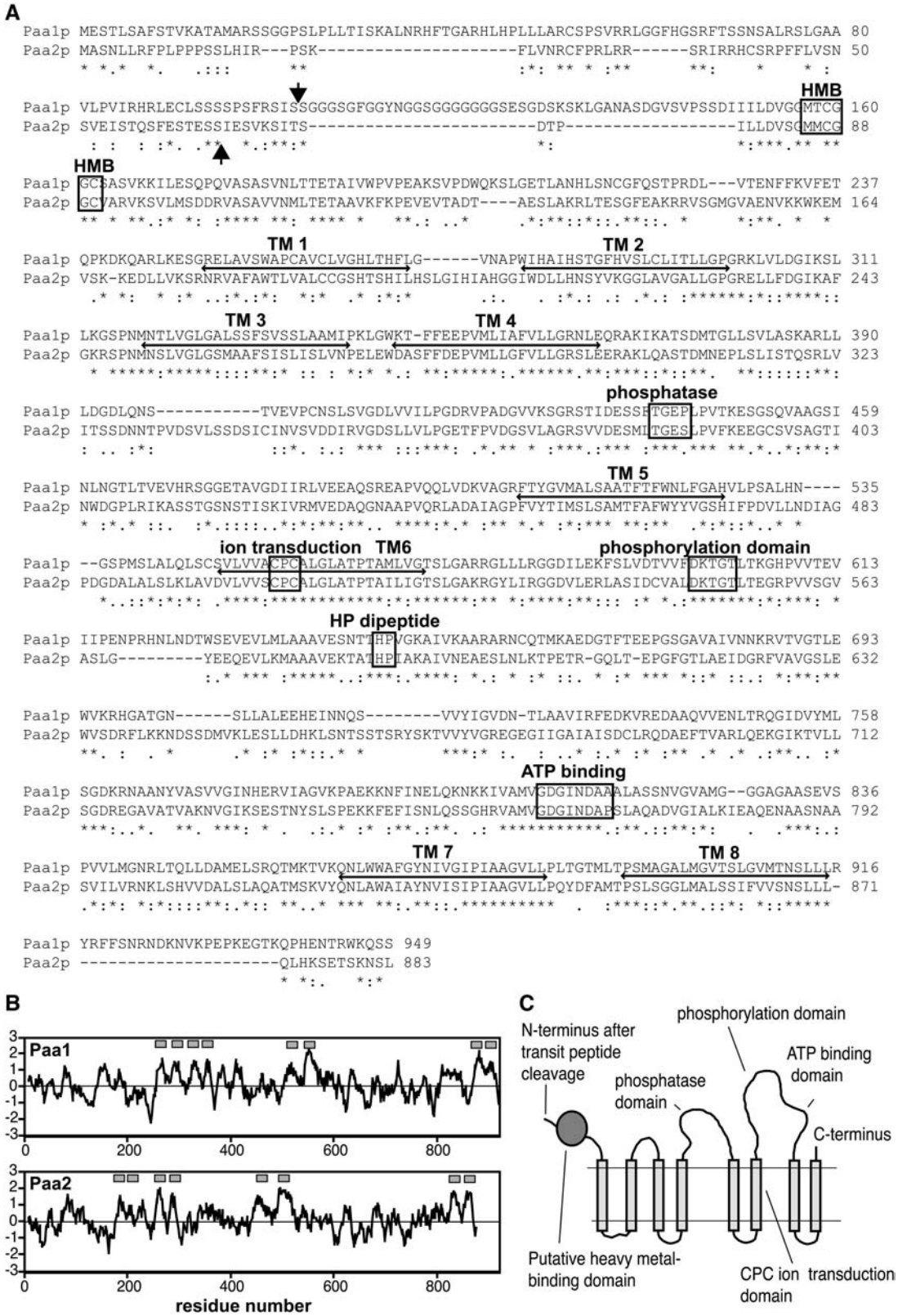

Figure 3. Sequence Comparison of the PAA1 and PAA2 Proteins.

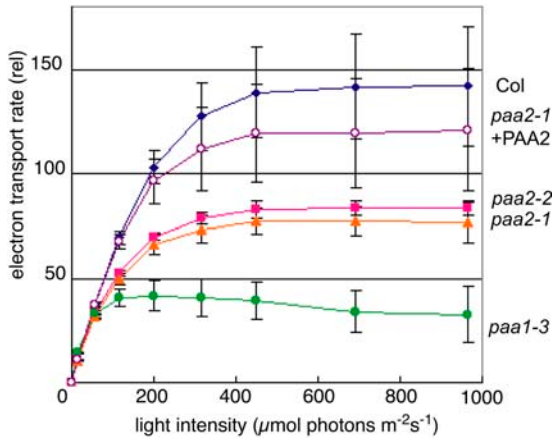

Figure 4. Light Intensity Dependence of Electron Transport Rate.

The relative electron transport rate was calculated from the product of Φ_{PSII} and light intensity ($\mu mol \cdot m^{-2} \cdot s^{-1}$). Φ_{PSII} is a chlorophyll fluorescence parameter representing the efficiency of PSII photochemistry (Genty et al., 1989). Each point represents the mean ± SD. The number of replicates is five for each line except for *paa2-1* + *PAA2*. *paa2-1* + *PAA2* represents *paa2-1* transformed by the wild-type *PAA2* sequence. Ten independent kanamycin-resistant seedlings were tested.

$CuSO_4$. By contrast, limitation of Cu availability (0.01 μM $CuSO_4$) further enhanced the phenotypes in both *paa1* and *paa2*. The effect of Cu on chlorophyll content was not as strong as on Φ_{PSII}, but the same trends were apparent. Thus, the *paa2* phenotype depends on Cu availability, but compared with *paa1* the effect of Cu is reduced.

Tolerance to excess Cu is a reported function of some Cu-transporting P-type ATPases (Kanamaru et al., 1994; Rensing et al., 2000). The Cu concentration of 50 μM is in the toxic range for Arabidopsis, at which visible growth defects such as reduced shoot size and root length are observed (data not shown) (Murphy and Taiz, 1995). This high Cu concentration affected both Φ_{PSII} and chlorophyll content in the wild type. Φ_{PSII} was comparable between the mutants and the wild type, whereas the chlorophyll content of *paa2* alleles was only slightly lower than those of the wild type and *paa1-4*, indicating that the sensitivity of Arabidopsis to this toxic level of Cu is not drastically affected in *paa2*, similar to *paa1* (Shikanai et al., 2003).

PAA2 Contains Chloroplast-Targeting Information

In vitro import experiments with pea chloroplasts have shown that the N terminus of the PAA1 precursor contains chloroplast-targeting information (Shikanai et al., 2003). The photosynthetic electron transport defect of *paa2* mutants suggested that the PAA2 protein is required for Cu delivery to plastocyanin in the thylakoid lumen, but to get to this location, Cu must cross several membranes. The TargetP program (Emanuelsson et al., 2000) predicted a chloroplast localization in the case of *PAA2* and a cleavable transit sequence of 65 amino acids. To examine the subcellular localization of the transporters, we constructed fusions with green fluorescent protein (GFP). The coding regions for the predicted chloroplast transit sequences of *PAA1* and *PAA2* were fused to *GFP*. Both transit sequence–*GFP* fusion constructs were expressed from a constitutive promoter in green Arabidopsis protoplast-derived cells. *GFP* alone expressed from the same promoter was used as a control. Because chloroplast transit sequences effectively mediate the translocation of a passenger protein across the envelope (Keegstra and Froehlich, 1999), the expected location for a GFP fusion to a transit sequence is the stroma. The localization in cells was analyzed using confocal laser microscopy. Fluorescence corresponding to GFP expressed without a transit sequence was excluded from the chloroplasts as expected, and comparison with bright-field images indicated that GFP was localized in the cytoplasm and in the nucleus (Figure 6A). By contrast, green fluorescence from the PAA1 transit sequence–GFP fusion and the PAA2 transit sequence–GFP fusion localized to the chloroplast, as indicated by the overlay of green fluorescence and red autofluorescence (Figures 6B and 6C). These results indicate that the N-terminal sequences of PAA2 and PAA1 function as chloroplast-targeting sequences. Therefore, the transporter proteins should function in the chloroplast either in the inner envelope membrane or in the thylakoids. For PAA1 protein, an envelope location had already been inferred from phenotypic analysis, but its location had not been demonstrated directly (Shikanai et al., 2003) in intact cells. To investigate directly in which membrane system PAA1 and PAA2 may function, we attempted to express full-length fusions with GFP. In contrast with the result obtained with the transit sequence fusion, the green fluorescence in cells expressing the full-length *PAA1-GFP* fusion was localized to the periphery of chloroplasts, consistent with localization in the envelope (Figure 6D). Because expression of the full-length fusion of *PAA2* to *GFP* never resulted in sufficient GFP signal, we could not localize the full-length PAA2. However, because topogenic information for membrane insertion may be contained in the first few transmembrane domains, we constructed additional fusions to GFP. To include the N-terminal parts of the precursor with the first and second predicted transmembrane regions, residues 1 to 301 of PAA1 were fused to GFP. For PAA2,

Figure 3. (continued).

(A) Sequence alignment of PAA1 and PAA2. Identical residues are indicated by stars, and similar residues are indicated by dots. The predicted transit sequence cleavage sites are indicated with vertical arrows. Functional regions of Cu-pumping P-type ATPases are indicated by boxes. HMB, putative heavy metal binding domain; TM 1 to TM 8, possible transmembrane regions. The GenBank accession numbers for PAA1 and PAA2 are BAA23769 and AY297817, respectively.

(B) Hydrophobicity profiles of PAA1 and PAA2. The scale of Kyte and Doolittle (1982) was used with a window of 15 residues. Hydrophobic regions are indicated by positive values. Gray boxes above each sequence indicate the putative transmembrane regions.

(C) Topology model of PAA2.

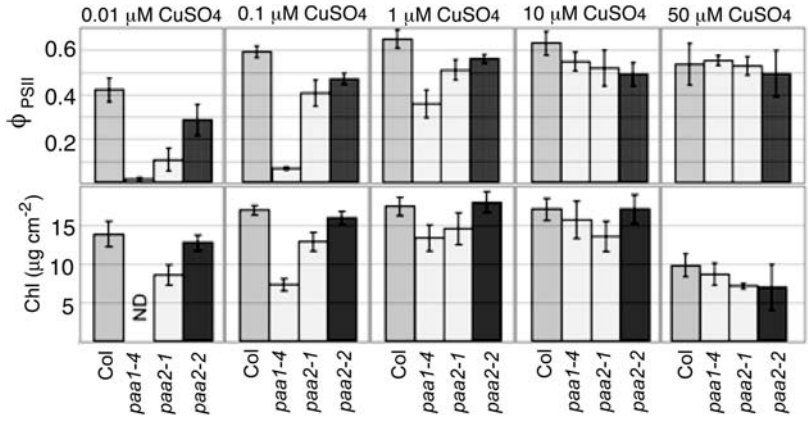

Figure 5. Response of *paa1* and *paa2* Plants to $CuSO_4$.

Both alleles of *paa2*, *paa1-4*, and the wild type (Col) were cultured on MS medium containing various concentrations of $CuSO_4$. The standard MS medium contains 0.1 μM $CuSO_4$. The response to Cu was evaluated by the chlorophyll fluorescence parameter Φ_{PSII} (efficiency of PSII photochemistry) at a light intensity of 200 $\mu mol \cdot m^{-2} \cdot s^{-1}$ and chlorophyll (Chl) content. *paa1-4* seedlings were too small to determine the chlorophyll content. Data are averages of five independent replicates. ND, not determined.

residues 1 to 306, including the first four predicted transmembrane domains, were fused to GFP. The localization results for these fusions are shown in Figures 6E and 6F. Green fluorescence in cells expressing the *PAA1/1-301-GFP* fusion was localized to the periphery of chloroplasts, consistent with the localization of the full precursor fusion (Figure 6E). This result indicates that envelope-targeting information for PAA1 is contained in the first two transmembrane domains. Interestingly, the location of the *PAA2/1-306-GFP* fusion seemed to overlap with the thylakoids, and no labeling of the chloroplast periphery was seen. These results suggest that PAA2 is not targeted to the envelope but instead may be targeted to the thylakoids.

To investigate localization by a different approach, we performed in vitro import experiments using isolated chloroplasts and in vitro translation of synthetic mRNA to obtain radiolabeled precursor proteins (Figures 7A and 7B). With this method, we did not succeed in the in vitro translation of full-length PAA2 (data not shown), as was the case for full-length PAA1 (Shikanai et al., 2003). However, after we introduced a stop codon that follows the codon for residue 333, we did observe translation resulting in a truncated precursor of the predicted size of 32 kD (Figure 7A, left gel, asterisk). This precursor includes the first four transmembrane domains. We analyzed the location of this protein by fractionation of the chloroplasts after in vitro import. We used the plastocyanin precursor as a control. The fractionation shows that the truncated PAA2 precursor is imported, resulting in a mature-sized protein after transit sequence fusion. The imported truncated PAA2 protein is protected from thermolysin protease treatment in the intact chloroplasts and fractionates with the membrane fraction, in which it is susceptible to protease treatment (Figure 7A, left gel), as would be expected for a thylakoid membrane protein. The control plastocyanin localizes to the thylakoid membrane fraction, in which it is fully protected from protease treatment (Figure 7A, right gel). To further investigate the suborganellar localization of truncated PAA2, the intact chloroplasts after thermolysin protease treatment (Figure 7A, left gel, fraction 2) were lysed and fractionated on a sucrose step gradient. The radiolabeled, imported protein was detected in the thylakoid fraction (Figure 7B, top gel), whereas no radioactive protein bands were detected in either stroma or envelope fractions. The separation and recovery of fractions was verified by immunoblotting using antibody markers specific for the stroma, thylakoids, and inner envelope membranes (Figure 7B, bottom three gels, respectively). We conclude from the data in Figures 6 and 7 and data obtained previously for PAA1 (Shikanai et al., 2003) that both the PAA1 and PAA2 proteins are active in chloroplasts. The data indicate that PAA1 functions in the envelope, whereas PAA2 is present in the thylakoid membrane. However, even though the data clearly indicate that the majority of the PAA1 and PAA2 proteins function in different membranes within the chloroplast, it cannot be excluded that a minor fraction of PAA2 could also be active in the envelope or a minor fraction of PAA1 could also be active in the thylakoids.

PAA2 Is Required for Cu Delivery to Thylakoids

A defect in *PAA1*, if the protein is active in the envelope, should affect Cu delivery to both the stroma and the thylakoids (Shikanai et al., 2003). Similarly, a defect in *PAA2*, if the protein is active in thylakoids, should result in altered metal ion levels in the chloroplast stroma and thylakoid lumen, which in turn may explain the photosynthesis phenotype of *paa2* alleles. To analyze directly whether *PAA2* is involved in Cu delivery to chloroplast compartments, we performed an elemental analysis of total leaf tissue and chloroplast fractions from wild-type and *paa2-1* plants and, for comparison, *paa1-3* plants. We did not observe a significant difference in the content of Cu, Fe, or Zn between leaves in wild-type and *paa2-1* plants (Table 1), indicating that PAA2 function is not required for metal ion delivery from the soil to the leaf tissue. However, a small but significant reduction was seen for the Cu content of *paa1-3* relative to wild-type plants. No significant differences were found for other measured elements in the leaf tissue (Mn, Mg, Ca, S, and P) among *paa2*, *paa1*, and

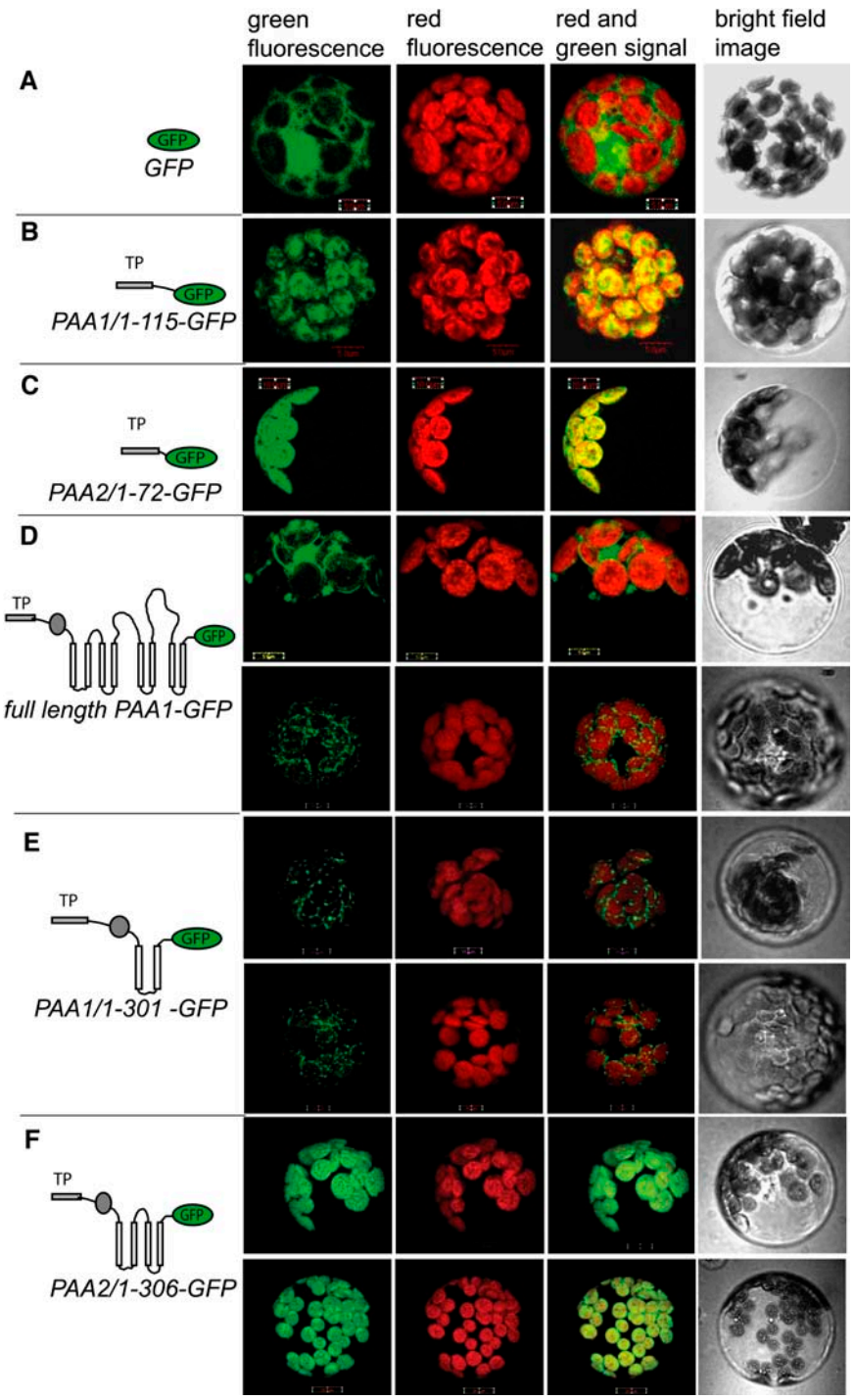

Figure 6. Subcellular Localization of PAA1 and PAA2.

Arabidopsis protoplasts were transformed with plasmids that express the indicated gene constructs under the control of the constitutive 35S *Cauliflower mosaic virus* promoter. The unfused *GFP* coding sequence served as a control. *PAA1/1-115-GFP* encodes the fusion of the *PAA1* transit peptide to the N terminus of *GFP*; *PAA2/1-72-GFP* is the fusion of the *PAA2* transit peptide to the N terminus of GFP. Full-length *PAA1-GFP* contains the full coding sequence of the *PAA1* precursor fused to GFP. *PAA1/1-301-GFP* is the fusion of the N-terminal part of the *PAA1* precursor, including the first two transmembrane domains, to GFP; *PAA2/1-306-GFP* is the fusion of the N-terminal part of the *PAA2* precursor, including the first four transmembrane domains, to GFP. After 16 h of expression, cells were observed using a confocal laser scanning microscope. Green fluorescence signals, chlorophyll red autofluorescence, an overlay of green and red signals, and bright-field images are shown.

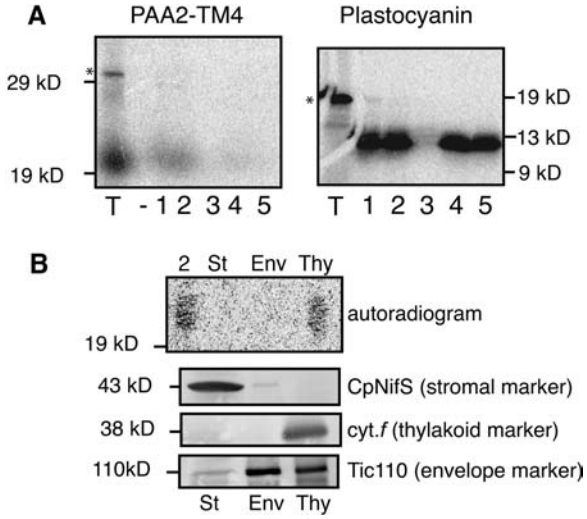

Figure 7. In Vitro Chloroplast Import and Fractionation.

(A) In vitro chloroplast import. PAA2-TM4 contains residues 1 to 333, including the first four transmembrane domains of PAA2. The precursor of plastocyanin was used as a control for import and fractionation. The radiolabeled precursor proteins in the translation mixture (T) were produced by in vitro translation in the presence of ^{35}S-Met and incubated with isolated pea chloroplasts. The translation mixture samples represent 10% of the precursor added to lanes 1 to 5. Precursor proteins of the expected sizes are indicated by asterisks. Chloroplasts were reisolated and proteins were either analyzed directly (lane 1) or after treatment with protease (lane 2). Protease-treated chloroplasts were lysed and further fractionated into a soluble fraction (lane 3) and a membrane fraction before (lane 4) and after (lane 5) protease treatment. Proteins were separated by SDS-PAGE, and the radiolabeled protein bands were visualized using a PhosphorImager.

(B) Sucrose gradient fractionation. Pea chloroplasts, after import and protease treatment (lane 2), were lysed in hypotonic buffer and fractionated into stroma (St), envelope (Env), and thylakoid (Thy) fractions by sucrose gradient centrifugation. Proteins were separated by SDS-PAGE and visualized using a PhosphorImager (autoradiogram) or blotted onto a nitrocellulose membrane and probed with the indicated antibodies.

the wild type (data not shown). As was noted previously (Shikanai et al., 2003), *paa1* chloroplasts had reduced Cu content compared with wild-type chloroplasts. Even though the Cu content of *paa2-1* chloroplasts was slightly lower than that of wild-type chloroplasts, this difference was not statistically significant. Interestingly, even though total Cu levels were comparable between wild-type and mutant leaf tissue, there was a large reduction of Cu content of the thylakoids for both mutants compared with the wild type. Whereas only a modest reduction was seen for Cu in the intact chloroplast of *paa2-1*, this line showed the most dramatic reduction of thylakoid Cu content (Table 1). These results indicate that *PAA2* has a role in Cu delivery to thylakoids. Fe levels were slightly but significantly increased in the intact chloroplast and the thylakoids of *paa2-1* (Table 1). Relative to the wild type, Zn levels were significantly increased in chloroplasts of both *paa1-3* and *paa2-1*, with the latter line showing the largest increase. Because there was no significant increase in the Zn levels of thylakoid fractions, the increases in chloroplast Zn levels in *paa1* and *paa2* may have been attributable to higher Zn concentrations in the stroma. These results support the role of PAA2 as a chloroplast-localized and most likely thylakoid-localized transporter specific for Cu.

paa1 and *paa2* Mutants Differ in Their Effect on the Activity and Expression of Chloroplast Cu Proteins

Two Cu proteins play important roles in photosynthesis in Arabidopsis. Plastocyanin is active in the thylakoid lumen, and CSD2 is active in the stroma. To investigate the role of PAA1 and PAA2 proteins in the biogenesis of these Cu proteins, we compared the abundance of plastocyanin (Figure 8) and SOD isoforms (Figure 9) in wild-type and mutant plants. A native gel electrophoresis assay (Li et al., 1990) was used to distinguish holoplastocyanin (with Cu bound) and apoplastocyanin (without Cu bound) isolated from the thylakoid lumen of wild-type and *paa2* plants grown on soil. Purified spinach plastocyanin, which is very similar in sequence to Arabidopsis plastocyanin, was used to identify bands corresponding to untreated holoplastocyanin and apoplastocyanin obtained after ascorbate and KCN treatment (Figure 8A, bottom two gels). In wild-type plants, plastocyanin was present in both the holo and apo forms (Figure 8A). However, a comparison of the staining intensities of both holoplastocyanin and apoplastocyanin on the control gel stained for total protein and the control immunoblot (Figure 8A) indicates that the antibody detects the apo form of plastocyanin with 5- to 10-fold better efficiency in this native gel assay. Thus, in wild-type thylakoids, the majority of plastocyanin is the holo form. In contrast with the situation in wild-type plants, and similar to what was found previously for the *paa1* mutants (Shikanai et al., 2003), plastocyanin was accumulated in the apo form in *paa2-1* and *paa2-2* mutants, and holo protein was hardly detectable (Figure 8A, top gel).

Apoplastocyanin in the thylakoid lumen may be unstable, as was found in Chlamydomonas (Li and Merchant, 1995). Indeed, the total amount of detectable plastocyanin polypeptide after separation on a denaturing gel in *paa1* and *paa2* mutants was much less than that in the wild type. A quantification of the band intensities in Figure 8B and replicate experiments indicates greater than 90% reduction of plastocyanin in both tested alleles of *paa1* and greater than 80% reduction in both alleles of *paa2* for plants grown on soil. The deficiency of plastocyanin in *paa2* mutants indicates that Cu delivery to the thylakoid lumen is severely impaired, which explains the observed defect in electron transport.

The electron transport defect was rescued by Cu feeding in both *paa1* and *paa2* mutants, but a much larger effect of Cu feeding was observed for *paa1*. To directly investigate the effects of Cu feeding on plastocyanin levels, plants were grown on MS-agar medium supplemented with different $CuSO_4$ concentrations or with the Cu chelator cuprizone (Figure 8C). Measurements of metal levels verified that Cu feeding increased total shoot Cu levels, whereas cuprizone decreased shoot Cu levels (data not shown). Because the results shown in Figures 8A and 8B indicate that total plastocyanin levels are a good indicator of holoplastocyanin levels, we analyzed plastocyanin in total leaf tissue by denaturing electrophoresis. As expected, Cu feeding or

Table 1. Metal Ion Profiles in Leaf and Chloroplast Fractions

Genotype	Fraction	Cu	Fe	Zn
Wild type	Leaf	15.7 ± 1.4[a]	102.7 ± 4.7[a]	94.6 ± 4.2[a]
paa1-3	Leaf	10.8 ± 0.8[b]	118.3 ± 11.5[a]	94.6 ± 3.6[a]
paa2-1	Leaf	13.1 ± 0.8[a,b]	98.4 ± 5.9[a]	99.5 ± 5.1[a]
Wild type	Chloroplast	0.50 ± 0.09[a]	4.06 ± 0.26[a]	2.97 ± 0.16[a]
paa1-3	Chloroplast	0.21 ± 0.03[b]	4.14 ± 0.13[a]	3.72 ± 0.27[b]
paa2-1	Chloroplast	0.42 ± 0.08[a,b]	6.46 ± 0.45[b]	4.51 ± 0.31[c]
Wild type	Thylakoid	0.15 ± 0.02[a]	1.49 ± 0.15[a]	0.23 ± 0.05[a]
paa1-3	Thylakoid	0.08 ± 0.01[b]	1.89 ± 0.21[a,b]	0.26 ± 0.04[a]
paa2-1	Thylakoid	0.01 ± 0.01[c]	2.31 ± 0.27[b]	0.21 ± 0.04[a]

Metal ion contents were measured for leaves of wild-type, *paa1-3*, and *paa2-1* plants grown on soil as well as for intact chloroplasts and thylakoids isolated from these plants. Values indicate amounts of metal ions (ppm or mg/kg dry weight for leaf fractions, μg/mg chlorophyll for intact chloroplast and thylakoid). All values are averages of three or four replicates ± SE. Superscripts indicate statistically significant groups (Student's *t* test; $P < 0.05$).

depletion affected plastocyanin levels in wild-type plants (Figure 8C), indicating that this protein is an important sink for Cu in green tissues, as had been noted (Marschner, 1995). However, the addition of toxic levels of Cu (50 μm) negatively affected plastocyanin accumulation in the wild type, an effect that is paralleled by a decrease in chlorophyll (Figure 5) and stunted plant growth (data not shown). Interestingly, plastocyanin content was partially rescued in the *paa1* mutant by increasing $CuSO_4$ concentrations (Figure 8C). This result suggests the presence of a Cu delivery pathway to plastocyanin, which functions independently of PAA1 at high shoot Cu levels. In contrast with what was observed for the wild type, supplementation with a toxic amount of Cu (50 μm) further increased the plastocyanin content in *paa1*. In the *paa2* mutants, we observed only a marginal increase in plastocyanin content with increasing $CuSO_4$ concentration (Figure 8C), and toxic amounts of Cu further reduced plastocyanin levels. RNA gel blot experiments indicated that plastocyanin transcription was not significantly affected by the Cu treatments and was comparable in wild-type and *paa1* and *paa2* plants (data not shown). The difference in plastocyanin accumulation in response to Cu between *paa1* and *paa2* supports the notion that PAA1 and PAA2 proteins function in different chloroplast membranes.

The quantitative analysis of the Cu content in *paa2-1* suggest that PAA2 protein functions as a Cu transporter in the thylakoids. If this is the case, *paa2* mutations should not have a negative effect on stromal Cu enzymes such as CSD2. To test this hypothesis, we analyzed the activity of SOD isozymes in leaf tissue from plants grown at different Cu concentrations (Figure 9A). The SOD isoforms can be distinguished by their mobility on native gels (Kliebenstein et al., 1998; Shikanai et al., 2003) and sensitivity to inhibitors (Bowler et al., 1992) (see Methods). The cytosolic CSD1 activity increased with Cu feeding in all plant lines (Figure 9A), but relative to wild-type plants it was more pronounced in *paa1* and *paa2*. Immunoblots (Figure 9B) and RNA gel blots (Figure 9C) indicate that increased CSD1 activity can be ascribed to an increase in gene expression.

The activity of stromal CSD2 was not detectable on the standard MS growth medium (0.1 μM $CuSO_4$) in the wild type but was detected in plants after Cu feeding (Figure 9A). Interestingly, increased CSD2 activity was observed for *paa2* compared with wild-type plants at all Cu concentrations, but the difference was especially clear at low Cu concentrations. In *paa1*, no CSD2 activity was observed for plants grown on MS medium containing 0.1 μM $CuSO_4$ (Figure 9A), but as with plastocyanin, very high Cu levels partially restored CSD2 activity. As with CSD1, the increase in CSD2 activity in response to Cu can be ascribed to an increase in gene expression, as increased CSD2 protein and mRNA levels were observed with increased Cu (Figures 9B and 9C). Quantification of the band intensities in Figure 9C indicates that in wild-type CSD2, mRNA levels are upregulated sevenfold at 5 μM Cu compared with 0.1 μM Cu. Similarly, *CSD2* expression is upregulated in *paa2* relative to the wild type at both the protein and mRNA levels (sixfold) when grown on the standard MS growth medium (0.1 μM $CuSO_4$). By contrast, the reduced CSD2 activity in *paa1* was not attributable to downregulation of gene expression; relative to the wild type, the *paa1* mutant had higher CSD2 polypeptide and mRNA levels at low Cu levels (0.1 μM $CuSO_4$) (Figures 9B and 9C). We conclude that in the *paa1* mutant, the SOD apoprotein, which is reported to be stable (Petrovic et al., 1996), accumulated in the stroma. Thus, the reduced activity of CSD2 in *paa1* is the result of a defect in Cu delivery.

To confirm the activity of CSD2, we analyzed SOD activities in stromal fractions prepared from isolated chloroplasts (Figure 9D). Intactness of the chloroplasts was indicated by the quantitative recovery of the stromal enzyme CpNifS, whereas purity was verified by the absence of the cytosolic marker P28 (Figure 9E). Analysis of the SOD activity in stromal fractions (Figure 9D) confirmed the increased presence of CSD2 activity in *paa2* and the decreased activity in *paa1*. The impaired delivery of Cu to the thylakoid lumen protein plastocyanin, together with an increase in the activity of the stromal Cu/ZnSOD in *paa2* mutants, strongly suggests that *PAA2* encodes a thylakoid Cu transporter. By contrast, the observed defects in Cu delivery to both stromal and lumenal chloroplast proteins (Figures 8 and 9) (Shikanai et al., 2003) suggest that PAA1 acts as a Cu transporter in the envelope.

The activity of MnSOD was the same in wild-type, *paa1*, and *paa2* plants under all conditions. However, two interesting

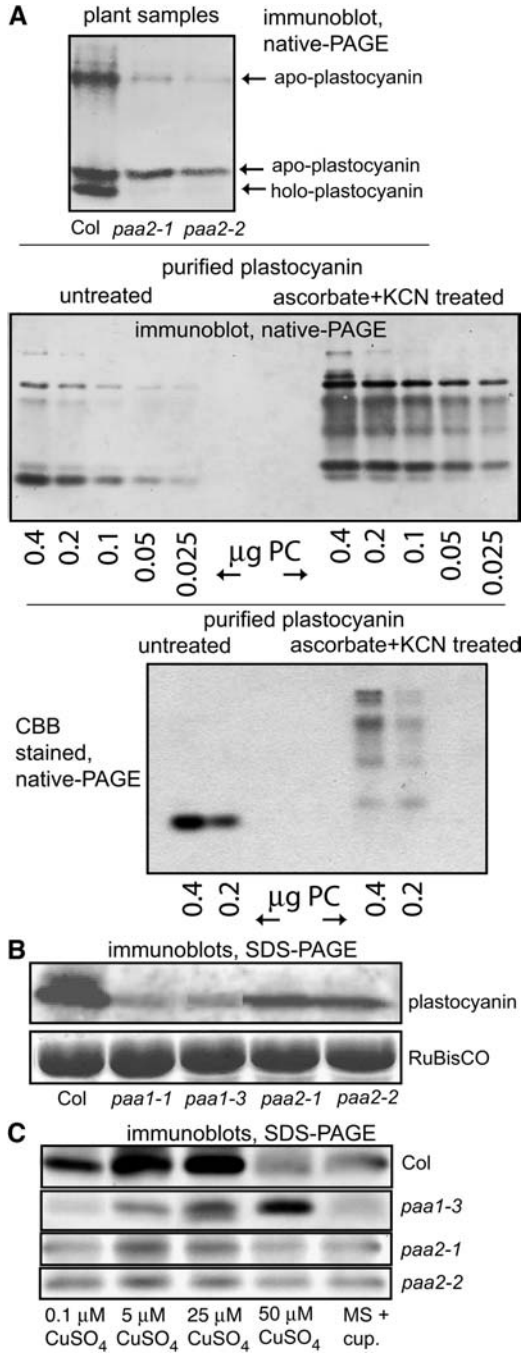

Figure 8. Analysis of Plastocyanin.

(A) Separation of apoplastocyanin and holoplastocyanin on native gels. The top gel shows soluble lumen proteins extracted from thylakoids equivalent to 3 μg of chlorophyll of the wild type (Col) and *PAA2* mutants separated on a 15% nondenaturing gel, blotted, and immunodetected with plastocyanin antibody. The bands were identified as either holoplastocyanin or apoplastocyanin by comparison with control native gels (middle and bottom gels) on which purified plastocyanin (PC) was present in either the holo form (untreated) or the apo form (ascorbate + KCN treated). Bands on the middle gel were immunodetected, whereas protein on the bottom gel was visualized by staining with Coomassie Brilliant Blue (CBB).

observations were made when examining stromal FeSOD activity. In wild-type plants, FeSOD activity was observed only on low Cu medium, and it was not detected in plants grown on Cu-supplemented medium (Figures 9A and 9D). Furthermore, compared with the wild type, we observed that stromal FeSOD activity was significantly reduced in *paa1* and slightly reduced in *paa2* (Figures 9A and 9D). The absence of FeSOD activity at high Cu and its reduction under low Cu conditions in the *paa1* and *paa2* mutants relative to the wild type can be explained by a reduction of FeSOD polypeptide levels (Figure 9B), which in turn can be ascribed to reduced mRNA levels (Figure 9C). Quantification of the data shown in Figure 9C demonstrated that on standard MS medium, FeSOD mRNA levels were reduced sixfold in *paa1* compared with the wild type. In *paa2*, this reduction was less than twofold.

The *PAA2* Transcript Is Present in Shoots, Whereas *PAA1* Is Expressed in Both Roots and Shoots

Photosynthesis is similarly affected in both *paa1* and *paa2* mutants. PAA1 is localized in the plastid envelope. On the other hand, the phenotypic analysis of *paa2* suggests a localization in thylakoids for PAA2. Thus, we may expect *PAA1* to be expressed in all tissues but *PAA2* to be expressed only in green tissue, in which the plastids develop into chloroplasts that contain thylakoids. We investigated the expression of *PAA1* and *PAA2* mRNA in root and shoot tissues by RT-PCR because the mRNA levels were too low to be detected on RNA gel blots. *PAA1* transcripts were detected in both shoot and root tissues, although we observed a much higher expression level in shoot tissue (Figure 10). On the other hand, *PAA2* transcripts were detected in the shoot only, and no products were detected in the root (Figure 10). Consistent with the localization data shown in Figure 6, these results suggest a role for PAA1 in both green and nongreen plastids, whereas PAA2 may function exclusively in green photosynthetically active chloroplasts.

The *paa1 paa2* Double Mutant Has a Seedling-Lethal Phenotype

To analyze the phenotype of double mutants, *paa2-1* was crossed with *paa1-4*. Genotypes of the resulting F2 progeny

(B) Analysis of total plastocyanin polypeptides. Proteins (20 μg) in total leaf homogenate of the wild type (Col) and the indicated mutants were separated by SDS-PAGE (15% gel), blotted, and immunodetected with either a plastocyanin antibody or the large subunit of ribulose-1,5-bisphosphate carboxylase/oxygenase (RuBisCO) antibody.

(C) Effect of Cu supplementation on plastocyanin levels in the wild type (Col) and *paa1* and *paa2* mutants. Arabidopsis seedlings were grown in MS medium supplemented with the indicated $CuSO_4$ concentrations or with the Cu chelator cuprizone (10 μM) for 3 weeks. Proteins (20 μg) in the total homogenate were fractionated by SDS-PAGE, blotted, and probed with plastocyanin antibody. Data shown are representative of at least two independent replicates.

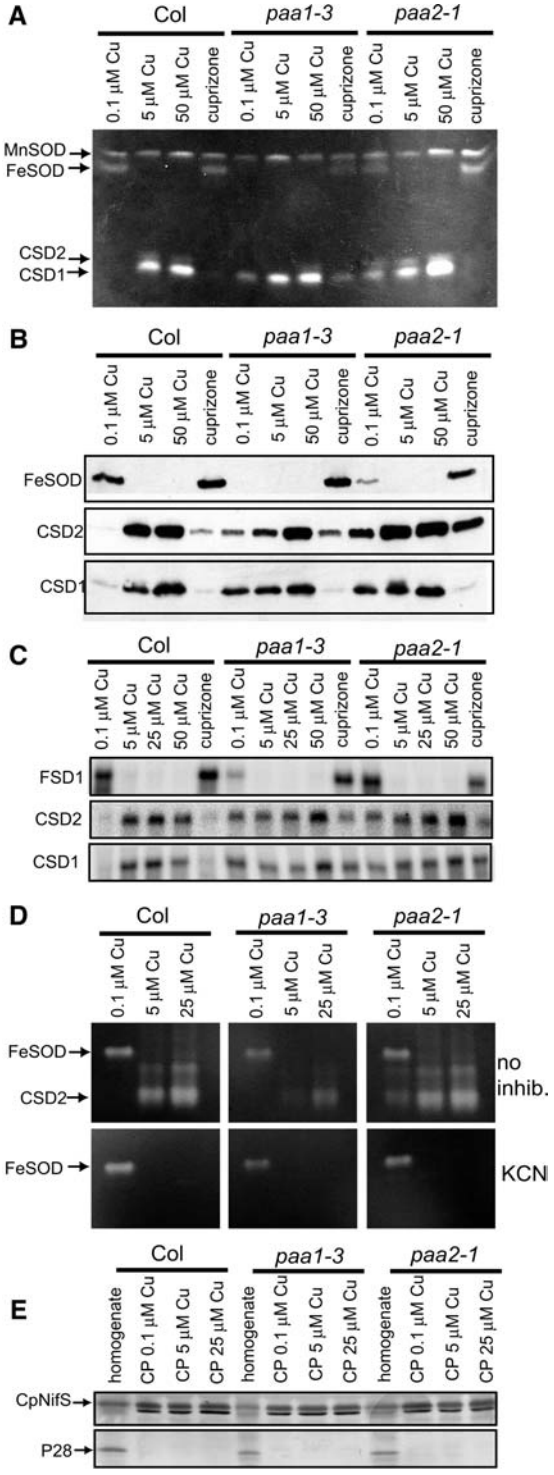

Figure 9. Analysis of SOD Isozyme Activity and Expression.

Wild-type (Col) and mutant seedlings were grown in MS medium supplemented with the indicated $CuSO_4$ concentrations or with the Cu chelator cuprizone (10μM) for 3 weeks.

(A) SOD isozyme activities in total shoot homogenate. Total soluble proteins (30 μg) were separated on nondenaturing 12% acrylamide gels, and the gels were stained for SOD activity.

were analyzed by PCR using primers designed to detect the *paa1-4* and *paa2-1* mutations. Among the F2 seedlings grown on soil, we found no double mutant homozygous for both *paa1-4* and *paa2-1* (data not shown). This result strongly suggests that the double mutant was lethal on soil. Because photosynthetic electron transport may have been severely affected in the double mutant, we tested the growth of the progeny of *paa1-4*/+ *paa2-1*/*paa2-1* on medium supplemented with sucrose to rescue the defects in photosynthesis caused by lesions. We compared growth on the standard medium (Figure 11, top) and MS medium supplemented with 5 μM $CuSO_4$, which was sufficient to at least partially suppress the defects in the single mutants (Figure 11, bottom). On standard MS medium containing 0.1 μM $CuSO_4$, *paa1-4* displayed a pale green leaf color and drastic reduction in growth rate (Figure 11, top) (Shikanai et al., 2003). Similarly, *paa2-1* seedlings also displayed some chlorosis (Figure 11), although the growth rate was unaffected. With Mendelian segregation, we expected one-fourth of the offspring of *paa1-4*/+ *paa2-1*/*paa2-1* to be homozygous for both recessive mutations. Indeed, seedlings with a growth phenotype that was much more severe than in either single mutant constituted approximately one-quarter of the total population (Figure 11, red arrows), whereas the other seedlings displayed a phenotype characteristic of *paa2-1*. PCR amplification of the *paa1* sequence confirmed that seedlings with this severe phenotype were homozygous for the *paa1-4* allele. The cotyledons in the double mutant were severely chlorotic, and true leaves did not emerge. The phenotypes were significantly more severe than those of *paa1-4*. This severe growth phenotype of the double mutant was evident in the light. In the dark, however, hypocotyl elongation and root growth were uniform among the progeny of *paa1-4*/+ *paa2-1*/*paa2-1* (data not shown).

On MS medium supplemented with 5 μM $CuSO_4$, the phenotype of *paa1-4* was drastically weakened (Figure 11, bottom). By contrast, the double mutants still displayed the severe growth phenotype and chlorosis. Although supplementation of the toxic

(B) Immunodetection of total SOD isoform polypeptides. Shoot proteins were fractionated by SDS-PAGE, and each SOD isoform was detected by immunoblotting using a specific antibody.

(C) SOD transcript levels. Ten micrograms of total RNA was separated by electrophoresis, transferred to Hybond N^+ membranes, and probed with ^{32}P-labeled gene-specific probes.

(D) Analysis of SOD activity in stromal fractions. Intact chloroplasts were isolated from Arabidopsis seedlings grown in MS medium supplemented with the indicated concentrations of $CuSO_4$. Stromal proteins (15 μg) were separated on 15% nondenaturing gels and stained for SOD activity. Gels were stained without inhibitor (no inhib.) or preincubated with KCN, which inhibits Cu/ZnSOD, to distinguish the activities of FeSOD and Cu/ZnSOD.

(E) Controls for chloroplast intactness and purity. Protein fractions of the total leaf homogenate of plants grown on MS medium and chloroplasts (CP) from plants grown on MS medium or MS medium with the indicated Cu concentrations were separated by SDS-PAGE and analyzed by immunoblotting. Fractions equivalent to 3 μg of chlorophyll were loaded. Immunoblots were probed with Arabidopsis CpNifS antibody as a stromal marker or with P28 antibody as a cytosolic marker. Data shown are representative of at least two independent replicates.

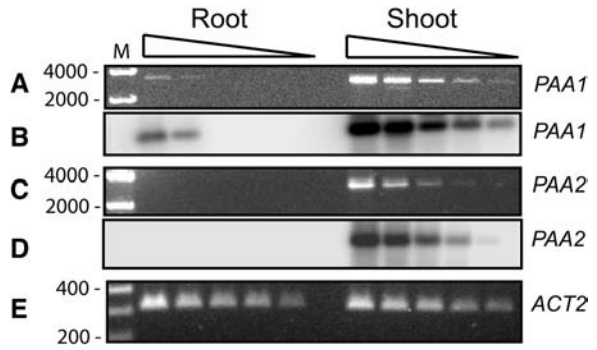

Figure 10. mRNA Expression of *PAA1* and *PAA2*.

One microgram of DNase-treated total RNA from either root or shoot was reverse-transcribed into cDNA. Serial dilutions from these cDNAs (left to right bands in each group: undiluted, 1:4, 1:16, 1:64, and 1:256) were used as templates for PCR using gene-specific primers for *PAA1*, *PAA2*, or the constitutively expressed actin (*ACT2*) gene as an internal control. Gels were stained with ethidium bromide (**[A]**, **[C]**, and **[E]**). PCR products were blotted and probed with gene-specific ^{32}P-labeled probes for *PAA1* **(B)** and *PAA2* **(D)**. The sizes of markers (M) are shown in base pairs.

level of Cu (50 μM) restored the leaf color, the growth rate was still severely affected in the double mutant (data not shown). We conclude that the *paa1 paa2* double mutant is seedling-lethal even on medium supplemented with sucrose.

DISCUSSION

Two Evolutionarily Conserved Cu Transporters in Chloroplasts

The Arabidopsis genome encodes for 46 P-type ATPases, the highest number identified to date among species with a completely sequenced genome (Baxter et al., 2003). Eight of these pumps, HMA1 to HMA8, can be classified in the heavy metal–transporting subfamily of P_{1B} pumps (Axelsen and Palmgren, 2001; Baxter et al., 2003). Phylogenetic analysis reveals that the eight Arabidopsis genes, together with *Oryza sativa* genes encoding P_{1B} pumps, fall into six clusters, and the genes in four of these clusters encode possible Cu transporters based on sequence similarity with known Cu pumps (Axelsen and Palmgren, 2001; Baxter et al., 2003). Arabidopsis has one possible Cu-transporting P-type ATPase in each cluster (HMA5, RAN1/HMA7, PAA1/HMA6, and PAA2/HMA8). The remaining Arabidopsis P_{1B} pumps show more similarity with Cd/Zn/Co/Pb-specific pumps from other organisms (Axelsen and Palmgren, 2001). Recent evidence indicates that HMA2, HMA3, and HMA4 function in Zn homeostasis and possibly cadmium tolerance (Mills et al., 2003; Gravot et al., 2004; Hussain et al., 2004). Among the putative Cu transporters, the gene product of *HMA5* is predicted to be functional in mitochondria, but functional characterization data are not available. The functions of RAN1 (Hirayama et al., 1999; Woeste and Kieber, 2000), PAA1 (Shikanai et al., 2003), and now PAA2 have been investigated, confirming a role in Cu transport.

Mutant alleles of *PAA2* were identified by positional cloning of high chlorophyll fluorescence mutants. The fluorescence phenotype could be ascribed to a defect in photosynthetic electron transport caused by insufficient formation of holoplastocyanin, which in turn was attributable to defects in Cu delivery to the thylakoid lumen. We propose a model in which *PAA1* functions in Cu transport across the plastid envelope and *PAA2* functions in Cu transport across thylakoids (Figure 12). The model is further corroborated by direct localization data and the tissue specificity of gene expression. Very strong support for the different localizations of PAA1 and PAA2 also comes from the phenotypic effects on Cu/ZnSOD activity and direct measurement of Cu levels in chloroplast compartments. However, at this time we cannot fully exclude dual localizations for both PAA1 and PAA2, even if these would represent only very minor fractions of the proteins.

Both the *paa1* and *paa2* mutants can be rescued partially by the addition of Cu to the plant growth medium, which in turn results in increased shoot Cu levels. Because some of the *paa1* and *paa2* mutants are effectively null alleles, the rescue may be explained by the presence of alternative low-affinity transport routes that function independently from PAA1 or PAA2 proteins. These transport activities may be explained by other unidentified

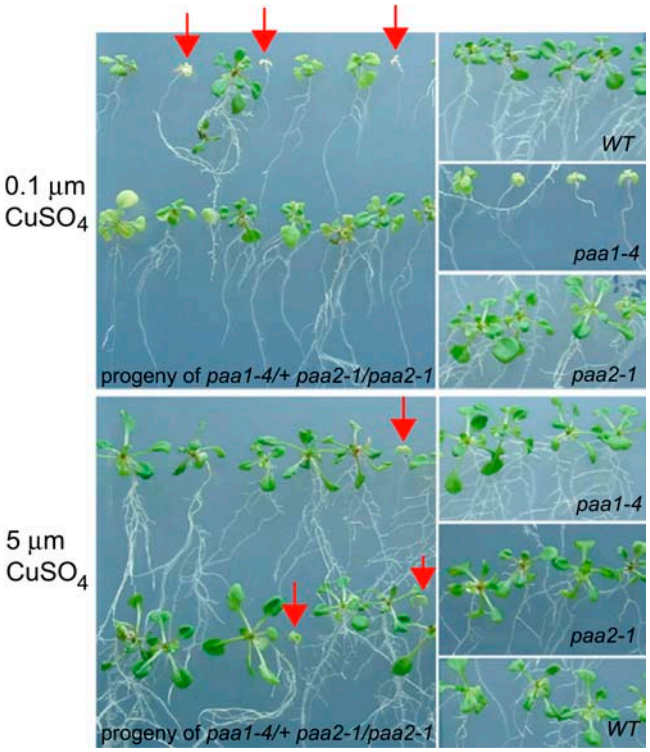

Figure 11. Seedling-Lethal Phenotype of *paa1 paa2*.

Progeny of *paa1-4*/+ *paa2-1*/*paa2-1* as well as the wild type (WT) and single mutants were cultured on MS medium containing 0.1 or 5 μM $CuSO_4$. *paa1-4 paa2-1* double mutants are indicated by red arrows. The genotype of the double mutants was confirmed by genome analysis using PCR.

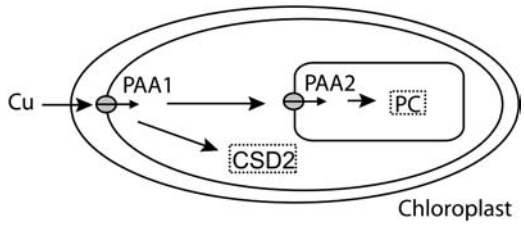

Figure 12. The Cu Delivery Systems in Plant Chloroplasts.

CSD2, stromal Cu/ZnSOD; PAA1 and PAA2, Cu-transporting P-type ATPases of Arabidopsis; PC, plastocyanin.

chloroplast-localized transporters, with lower affinity and maybe broader specificity. We still have a lot to learn about the identities of ion transporters in the chloroplast envelope for trace metals, and this is an interesting area of research for the future. One approach that we are taking is to screen for suppressors of the *paa1* mutants. The extreme Cu-chelating capacity of cells (Rae et al., 1999) suggests that Cu delivery must be mediated specifically by proteins at all times. The bacterium *Escherichia coli* has several extrusion mechanisms to prevent Cu accumulation in the cytosol, but an import system for Cu has not been described (Rensing and Grass, 2003). Therefore, it has been suggested that Cu, particularly Cu(I), may be transported with low efficiency into the bacterial cytosol by passive transport systems with low specificity (Outten et al., 2001). Notably, increased Cu had a more dramatic effect on plastocyanin levels in *paa1* compared with *paa2* (Figure 8). The increased pH in the stroma, relative to the cytosol, should establish an electrochemical gradient that would favor the transport of positively charged Cu ions by a low-specificity pathway in *paa1*, particularly in the light. By contrast, the electrochemical gradient over the thylakoid membrane would not favor the transport of Cu ions across thylakoids in *paa2*. In the *paa2* mutant, some plastocyanin is found in the holo form, even on low Cu. With regard to this finding, it is interesting that energy-independent transport of Cu(II) in thylakoid membranes of peas was measured using an assay that uses a fluorescent Cu-sensitive probe (Shingles et al., 2004). The components responsible for this activity have not been identified. Because the membranes that were used to observe Cu transport were obtained by differential centrifugation (Shingles et al., 2004), the presence of other cellular membranes cannot be excluded completely (Peltier et al., 2002; Friso et al., 2004); therefore, the physiological relevance will become more clear after all involved components are identified.

In cyanobacteria, which are believed to share a common evolutionary ancestry with chloroplasts, two P-type ATPases, CtaA and PacS, function in Cu transport (Kanamaru et al., 1994; Phung et al., 1994). CtaA is most likely located in the cell membrane and required for Cu uptake in the cell (Phung et al., 1994; Tottey et al., 2001), whereas PacS is located in cyanobacterial thylakoids and required for Cu transport to the lumen and Cu tolerance by extrusion of Cu from the cytosol (Kanamaru et al., 1994; Tottey et al., 2001). Thus, *PAA1* and *PAA2* can be considered functional homologs of *CtaA* and *PacS*, respectively, and key components of the Cu delivery system to plastocyanin are conserved between cyanobacteria and chloroplasts. Similarly, upon import into the stroma, the sorting signal that is used for translocation of the plastocyanin polypeptide across thylakoids is conserved between plants and cyanobacteria (Smeekens et al., 1986). Indeed, both plastids and cyanobacteria use a SecA/SecY-mediated pathway to target plastocyanin to the thylakoid lumen (for review, see Schnell, 1998). Thus, in the biogenesis of plastocyanin, both the polypeptide and the cofactor make use of conserved membrane transport pathways.

Our experiments indicate that PAA1 is targeted to the envelope, whereas PAA2 functions in thylakoids. Thus, there should be different targeting information present in both proteins. The available evidence indicates that this information is present in the N-terminal regions. However, for the PAA2 localization, we could use only truncated proteins, so other parts of PAA2 could also have targeting information, which may be tested in the future. At present, we do not know which machinery targets the PAA1 and PAA2 proteins to their locations in chloroplasts. The CpSRP pathway is responsible primarily for the insertion of light-harvesting complex proteins in thylakoid membranes (Asakura et al., 2004), but other integral membrane proteins use a separate pathway (for review, see Schnell, 1998). Recently, it was found that a poly-Gly stretch, which follows a transit sequence, may serve as a signal for envelope retention for an outer envelope protein when it follows a canonical transit sequence that targets proteins to the stroma (Inoue and Keegstra, 2003). Interestingly, PAA1 but not PAA2 contains a poly-Gly stretch located between the transit sequence and the heavy metal binding domain (Figure 3), and this motif may play a role in PAA1 targeting.

In cyanobacteria, PacS acquires Cu from a molecular chaperone, bacterial Atx, a small protein with a CxxC metal binding motif (Tottey et al., 2002). Bacterial *Atx* is similar to yeast *ATX* (Lin et al., 1997; Pufahl et al., 1997) and plant *CCH* (Himelblau et al., 1998). We have searched the Arabidopsis genome for a gene encoding a protein with similarity to bacterial or eukaryotic Atx and with a possible predicted chloroplast location. Except for one close homolog of *CCH* that we confirmed to be cytosolic (S.E. Abdel-Ghany, J. Burkhead, and M. Pilot, unpublished data), we found no possible plastidic *ATX* homolog. In this respect, it is worth noting that our screens for photosynthesis mutants, which in retrospect selected strongly for plants with defects in plastocyanin, resulted in eight alleles of Cu-transporting P-type ATPase genes, but no other Cu-targeting genes were identified in this way. In plants, Cu is delivered to stromal CSD2 as well as PAA2 and plastocyanin. Cu/ZnSOD enzymes are thought to have originated in the Eukarya (Bowler et al., 1992) and are absent from cyanobacteria (Raven et al., 1999). Thus, compared with cyanobacteria, Cu has a new target in the chloroplast.

Responses to Cu in the Chloroplast

FeSOD and Cu/ZnSOD are two structurally unrelated enzymes (Bowler et al., 1992), and the FeSOD (*FSD1*) and Cu/ZnSOD (*CSD1* and *CSD2*) genes in plants differ somewhat in their regulation in response to various oxidative stresses (Kliebenstein et al., 1998). Our data show that the expression of both genes is most dramatically regulated by Cu, which suggests an important role of Cu in the regulation of oxidative stress protection. In the wild type, *FSD1* expression is upregulated under low Cu

conditions, and its regulation is reciprocal with that of *CSD2*, which is downregulated on low Cu medium (Figure 9). However, under these low Cu conditions, an additional subtle regulation of the SOD genes is apparent when comparing the wild type and *paa1* and *paa2* mutants. In plants grown on MS medium or MS plus cuprizone, we observed that *FSD1* expression was again downregulated with a concomitant upregulation of *CSD2* in both *paa1* and *paa2* compared with the wild type (Figure 9). PSI is a major site of superoxide formation in plants, and the acceptor (stromal) side of PSI is where SOD enzymes should be active (Asada, 1999). It has been reported that methyl viologen, which promotes the formation of superoxide, enhances FeSOD expression, an effect that is reversed by adding the PSII inhibitor DCMU (Tsang et al., 1991). A reduction in plastocyanin should diminish the amount of reactive oxygen species formed at PSI. Therefore, the downregulation of *FeSOD* expression in *paa2* on low Cu may be in response to the amount of reactive oxygen species generated at the acceptor side of PSI, as had been suggested for *paa1* mutants (Shikanai et al., 2003). The more dramatic downregulation of *FSD1* in *paa1* compared with *paa2* is consistent with the differences in electron transport and plastocyanin levels in these mutants. The plastid-derived signal affecting the expression of nucleus-encoded SOD isoforms under low Cu conditions could be related directly to chloroplast-localized oxidative stress (Tsang et al., 1991) or the reduction state of the plastoquinon pool (Escoubas et al., 1995).

Relative to the wild type, the Zn levels in chloroplasts isolated from soil-grown *paa1* and *paa2* plants were increased, particularly in *paa2* plants. At least for *paa2* plants, this increased Zn level may be a reflection of the higher expression of the stromal Cu/ZnSOD, which may create a larger sink for Zn in the stroma. The Fe levels in chloroplast fractions isolated from soil-grown *paa2* plants, but not *paa1* plants, were increased significantly relative to those in wild-type plants. The reason for this increase in Fe is unclear at this time.

Cu only becomes limiting to photosynthesis at a concentration of less than 0.1 μM (Figure 5). At this concentration, plastocyanin was the major Cu protein detectable in leaf tissue (Figures 8 and 9), indicating a preferential delivery of Cu to the thylakoid lumen under conditions of low Cu supply. Although Cu is essential to various cellular functions, excess Cu is toxic (Nelson, 1999). Therefore, plants must not only have systems for Cu delivery, which allow Cu to be delivered to where it is most needed under conditions of low supply, but should also respond to a possible excess of Cu. As plants are grown at the subtoxic concentrations of 5 to 25 μM Cu, the amounts of major Cu proteins, plastocyanin in the thylakoid lumen, CSD2 in the stroma, and CSD1 in the cytosol, all increase (Figures 8 and 9). The increases in the Cu/ZnSOD proteins were attributable to increased transcript levels. The observed increase in plastocyanin in plants grown at greater than 0.1 μM Cu was not linked to an increase in electron transport activity (Figures 5 [Φ_{PSII}] and 8). Thus, plastocyanin and the Cu/ZnSOD proteins together may serve to buffer excess Cu. When plants were grown on toxic Cu levels (50 μM Cu), the amount of plastocyanin severely decreased again in wild-type plants. The decrease in plastocyanin at toxic Cu levels was accompanied by a decrease in chlorophyll and may have been caused by damage to the thylakoids, as the amounts of Cu overwhelm the cell's buffering capacity. These responses to Cu seemed preserved or even exaggerated in the *paa2* mutants. However, the response to excess Cu was altered in *paa1*, in which plastocyanin levels were highest at 50 μM Cu. The thylakoid membrane of *paa1* mutants should be more protected from excess Cu caused by the lack of Cu transport into the stroma.

The toxic effect of Cu on the photosynthetic machinery can be counteracted by the buffering effect of Cu binding by CSD1 and perhaps metallothioneins in the cytosol, but particularly by CSD2 in the stroma. With respect to this fact, it is very interesting that relative to the wild type, the *CSD2* transcript levels are increased in *paa2*, which accumulates more Cu in the stroma. By contrast, *CSD2* transcript levels are decreased at least at intermediate Cu concentrations in *paa1*, which accumulates less Cu in the stroma. These observations suggest that Cu is sensed in the stroma of the chloroplast and that this signal influences transcript levels of the nucleus-encoded *CSD2* gene. Thus, metal homeostasis in Arabidopsis involves communication between the chloroplast and the rest of the cell, which is partly disturbed in *paa1* and *paa2* mutants.

The Significance of Cu Delivery for Photosynthesis in Plants

The mild reduction in electron transport observed for *paa2* is similar to what was observed for *protein gradient regulation1* (*pgr1*), a mutant of the cytochrome b_6f complex (Munekage et al., 2001), and both *paa2* and *pgr1* have growth rates that are similar to that of wild-type plants. Compared with *paa2*, the growth phenotypes of *paa1* mutants were more severe, which can be ascribed to more reduced plastocyanin levels and the lack of stromal Cu/ZnSOD activity in green tissue. It is also possible that the *paa1* phenotype is caused by defects in Cu homeostasis in nongreen plastids, because *PAA1* is expressed in roots as well as in green tissues (Figure 10). However, seedling growth of *paa1* was not affected in the dark on medium supplemented with sucrose (data not shown). This observation, together with the more severe defect in electron transport and the reduction in chlorophyll content, suggest that the lack of plastocyanin and SOD proteins in green plastids is responsible for the more severe phenotype of *paa1*.

We observed that the *paa1 paa2* double mutant was seedling-lethal; although germination was observed on sucrose medium, the plants died as seedlings. The most straightforward explanation for this phenotype is a very severe inhibition of Cu delivery to plastocyanin, which is the only protein that can accept electrons from the cytochrome b_6f complex in vitro (Molina-Heredia et al., 2003). Indeed, plants with insertions in both plastocyanin genes are seedling-lethal on soil (Weigel et al., 2003). Intriguingly, the phenotype of *paa1 paa2* seems to be more severe than that reported for plants without plastocyanin, because it was reported that it is possible to maintain plastocyanin-less plants on sucrose medium (Weigel et al., 2003). An important difference between plastocyanin-less plants and the *paa1 paa2* double mutant may be Cu delivery to stromal Cu/ZnSOD and thus the capacity to scavenge reactive oxygen species. In this respect, it is of interest that the phenotype of *paa1 paa2* was influenced by light. Interestingly, Arabidopsis knockdown mutants for *CSD2*

were reported to display a very severe and light-dependent growth phenotype (Rizhsky et al., 2003), seemingly even more severe than that of *paa1* mutants (Figures 1, 5, and 11). Even though the phenotype of *paa1* may be more severe than that of *paa2*, it may be less severe compared with a *CSD2* knockdown mutant, because in *paa1* mutants Cu delivery to both stromal SOD and plastocyanin are affected simultaneously. The reduced activity of plastocyanin may diminish the need for reactive oxygen species scavenging via an active water–water cycle, because PSI will be more oxidized.

For optimal photosynthesis and optimal use of available metal ions, the chloroplast may need to balance the activity of lumenal plastocyanin and stromal SOD enzymes under various conditions of metal supply. The regulation of genes for stromal SOD enzymes and the plastid Cu delivery system together seem geared to achieve this dual goal. On low Cu medium, wild-type plants still produce active plastocyanin, whereas SOD activity is provided by FeSOD alone (Figure 9). The shutoff of *CSD2* under these low Cu conditions could make it easier for PAA2 to deliver Cu to plastocyanin in the lumen, particularly if a specialized Atx-like Cu chaperone is absent. When Cu supply is sufficient, *CSD2* is transcribed and no FeSOD is active, possibly saving Fe for other uses. In these conditions, a balanced delivery of Cu to plastocyanin via PAA2 and to stromal Cu/ZnSOD must ensure that there is enough SOD activity to deal with the reactive oxygen species formed at PSI. As Cu supply is increased, more Cu/ZnSOD accumulates in the stroma, with a concomitant increase of plastocyanin in the lumen. However, the increase in CSD2 seems more dramatic, suggesting a preferential delivery of Cu to CSD2 over the pathway to plastocyanin via PAA2, which may be less favored because of the lack of an Atx-like protein. Under high-Cu growth conditions, both plastocyanin and stromal Cu/ZnSOD may help to buffer Cu concentrations, as has been reported for yeast Cu/ZnSOD (Culotta et al., 1995). In the *paa2* mutant defective in electron transport, this may be the most important role for *CSD2*.

METHODS

Plant Materials, Growth Conditions, and Map-Based Cloning

The background of *Arabidopsis thaliana paa2-1* and *paa2-2* is Col *gl1* (Col-3). Both alleles were derived by mutagenesis with ethyl methanesulfonate. The *paa1* alleles used in this study were *paa1-3*, which is in the Col-0 background, and *paa1-4*, which is in the Col-3 background, and have comparable phenotypes (Shikanai et al., 2003). Plants were grown in Metromix potting soil under controlled conditions (light intensity of 40 $\mu mol \cdot m^{-2} \cdot s^{-1}$, 16-h/8-h light/dark cycle at 23°C). For chloroplast isolation and extraction of plastocyanin, larger numbers of plants were grown in a greenhouse with natural sunlight supplemented by lighting from sodium lamps to give 15 h of light during the photoperiod. For growth on agar medium, seeds were surface-sterilized and sown on agar-solidified MS medium including 3% sucrose (Sigma-Aldrich, St. Louis, MO). The medium was supplemented with $CuSO_4$ or the chelator cuprizone (Sigma number C9012) as indicated.

The *paa2-2* mutation was mapped with cleaved amplified polymorphic sequence markers (Konieczny and Ausubel, 1993). Genomic DNA was isolated from F2 plants derived from the cross between *paa2-2* and the polymorphic wild-type Landsberg *erecta*. Primer sequences and restriction enzymes used for mapping were 5′-TCATGCATCAAAAACCGACAG-3′ and 5′-TAATCCTGGACACAAGAATCC-3′ (*Hin*dIII [T10F18]) and 5′-GTCTTGTTCATGTGAAACTGC-3′ and 5′-TGATTGATTCTTTAGCCATCG-3′ (*Mse*I [MWD9]). Genomic *PAA2* sequences containing the wild type and both *paa2* alleles were amplified by PCR using Ex-Taq DNA polymerase (Takara, Kyoto, Japan). Resulting PCR products were sequenced directly using a dye terminator cycle sequencing kit and an ABI prism 3100 sequencer (Perkin-Elmer, Norwalk, CT).

For complementation of the *paa2-2* mutation, the 6.8-kb fragment containing the wild-type *PAA2* sequence flanked by 5′-TCTAGATGTGTTGTAGAAGA-3′ and 5′-AAGCTTCCTCCGTTGTATCC-3′ (complementary) was cloned in pBI101. The resulting plasmid was introduced into the *Agrobacterium tumefaciens* pMP40 strain and then transformed (Clough and Bent, 1998) into *paa2-2*.

Plasmid Construction

Total RNA from root and shoot was isolated using TRIzol reagent (Invitrogen, Carlsbad, CA). First-strand cDNA was synthesized from 1 μg of DNase1-treated total RNA using *Moloney murine leukemia virus* RT (Promega, Madison, WI) and oligo(dT) primers according to instructions. The Expand polymerase enzyme kit (Roche Diagnostics, Indianapolis, IN) was used to amplify the *PAA2* coding sequence using the flanking primers *Sma*I–N-ter (5′-TCCCCCGGGATGGCGAGCAATCTTCTCCGATTT-3′) and *Xho*I–C-ter (5′-CGGGCCTCGAGAATAGATGTGGAGCCGATCACAAG-3′) by PCR. The underlined sequences are the restriction sites. The amplified product was digested with *Sma*I and *Xho*I, cloned into pBluescript KS+ (Stratagene, La Jolla, CA), and sequenced by the dideoxy dye termination method. The cDNA sequence was deposited in the GenBank database with accession number AY297817.

The *GFP* reporter plasmid 35Ω-SGFP(S65T) was generously provided by Norbert Rolland (Universite Joseph Fourier, Grenoble, France). Construction of the plasmids for expression of fusions to *GFP* was as follows. The transit sequence of *PAA1* (amino acids 1 to 115) and the transit sequence of *PAA2* (amino acids 1 to 72) were amplified by PCR using flanking primers *Sal*I–N-ter (5′-GAATGGTCGACATCGAGAGATTGATCGAGAGATTGAGATTACGGAGC-3′) and *Nco*I–C-ter (5′-CATGCCATGGCACCATTATACCCCCCAAATCCAGAA-3′) for *PAA1* and *Sal*I–N-ter (5′-GAATGGTCGACTACATCGCGTGACTATCGTCGTCTGT-3′) and *Nco*I–C-ter (5′-CATGCCATGGTAATGGATTTCACAGATTCGATTGAAG-3′) for *PAA2*. The N-terminal primers hybridize to the 5′ untranslated region. Genomic DNA was used as the template for PCR. PCR products were inserted into the *Sal*I–*Nco*I-digested GFP reporter plasmid to create PAA1/1-115-GFP and PAA2/1-72-GFP. Similarly, the PAA1/1-301-GFP fusion was constructed after PCR using primers PAA1.N-ter.Sal 1 (5′-GATCGTCGACATGGAGTCTACACTCTCAGCT-3′) in combination with PAA1.Rev. Nco1 3 (5′-CATGCCATGGGTACAGGACCAAGCAACGTAA-3′). The fusion of PAA2/1-306-GFP was constructed after PCR using primers PAA2.N-ter.Sal 6 (5′-ACGCGTCGACATGGCGAGCAATCTTCTCCGATT-3′) and PAA2TMD4R (5′-ACGCGTCGACAGATGCTTGAAGCTTTGCTCTTT-3′). The orientation was confirmed by restriction digestion and sequencing. For the latter two fusions, cDNA clones were used as templates for PCR. To make a fusion with GFP of the full-length PAA1, the entire coding sequence was amplified by PCR using flanking primers PAA1.N-ter.Sal 1 and *PAA1-rev-Sal*I (5′-ACGCGTCGACAGAGCTTTGCTTCCATCTTGTGTT-3′). The PCR products was inserted into the *Sal*I-digested GFP plasmid to create PAA1/FL-GFP. The correct orientations of the insertion and fusion of full DNA sequences were verified by sequencing using the dideoxy method. The plasmids used for protoplast transformation were prepared using the Plasmid Midi Kit (Qiagen, Valencia, CA). Construction of the plasmid for in vitro transcription of a truncated *PAA2* was performed as follows. The *PAA2* precursor sequence including the first four transmembrane domains was

amplified by PCR using primers *Sma*I–N-ter (described above) and PAAHR5 (5′-CGGGCCTCGAGTTACAGAATCCACTGGGGTGT-3′). The amplified product was digested with *Sma*I and *Xho*I and cloned into pBluescript KS+ (Stratagene). Plasmid was linearized by *Kpn*I and in vitro transcribed using T7 polymerase. The vector used for in vitro transcription of the plastocyanin sequence from *Silene pratensis* was as described (Smeekens et al., 1986).

Subcellular Localization of GFP Fusion Proteins

GFP fusions were expressed in Arabidopsis protoplast derived cells from the 35S promoter in the GFP reporter plasmid 35Ω-SGFP(S65T). For protoplast preparation, Arabidopsis plants (ecotype Col) were grown on MS medium for 3 weeks. Two grams fresh weight of leaf tissue was suspended in 30 mL of a buffer containing 1% (w/v) cellulase Onozuka R-10, 0.25% Macerozyme R-10 (Karlan Research Products, Santa Rosa, CA), 8 mM $CaCl_2$, 0.5 M mannitol, and 5 mM Mes, pH 5.5, vacuum infiltrated for 1 min, and incubated for 3 h at room temperature with gentle shaking. The clear digest was filtered through a 37- to 70-μm nylon mesh (Carolina Biological Supply, Burlington, NC), and the protoplasts were harvested by centrifugation for 5 min at 1000 rpm and washed twice in 10 mL of W5 wash solution (154 mM NaCl, 125 mM $CaCl_2$, 5 mM KCl, 5 mM glucose, and 0.5 M mannitol, adjusted to pH 5.8 with KOH). The pellet was suspended in ~2 mL of mannitol/Mg solution (15 mM $MgCl_2$, 0.4 M mannitol, and 0.1% Mes, pH 5.6). Protoplasts were counted using a hemocytometer, and their concentration was adjusted to 3×10^6 cells/mL with mannitol/Mg solution. Fifty micrograms of plasmid DNA, 100 μg of salmon sperm DNA, and 300 μL of polyethylene glycol solution [40% polyethylene glycol 6000, 0.4 M mannitol, and 0.1 M $Ca(NO_3)_2$, adjusted to pH 8.0 with KOH] were added to 300 μL of the protoplast solution, very gently mixed, and left for 30 min at room temperature. The solution was very slowly diluted with 10 mL of W5 solution and then pelleted by centrifugation for 5 min at 1000 rpm. Protoplasts were further resuspended in 5 mL of protoplast culture medium composed of MS medium supplemented with 0.4 M glucose, 0.4 M mannitol, 1 mg/L 2,4-D, and 0.15 mg/L kinetin, pH adjusted to 5.8 with KOH, and left at 23°C for 16 h under continuous light. Confocal images were obtained using an Olympus Fluoview 300 inverted confocal laser scanning microscope (1X70) equipped with an argon ion laser system and a 1.4-numerical aperture 60× objective lens (Olympus America, Melville, NY). In all experiments, the microscope stage was maintained at room temperature. The fluorescence signals were detected at 530 nm for GFP and 660 nm for chlorophyll. Sections of 1-μm thickness were scanned, and images were captured with the Fluoview software as Tiff files. Eight sections were superimposed, and images were imported into Adobe Photoshop (Mountain View, CA) and cropped.

In Vitro Chloroplast Import Assays and Fractionation

Radiolabeled precursors were synthesized in a wheat germ lysate system in the presence of ^{35}S-Met (25 μCi/50 μL reaction) (Amersham/Pharmacia, Piscataway, NJ) according to suggested protocols (Promega). After translation, unlabeled Met was added to 5 mM and postribosomal supernatants were prepared by centrifugation at 100,000*g* at 4°C for 20 min. The radiolabeled precursors were incubated with chloroplasts that were isolated from 10-d-old pea seedlings (*Pisum sativum* cv Little Marvel) as described (Pilon et al., 1992). The postimport thermolysin treatment and reisolation of intact chloroplasts as well as fractionation into stromal and crude membrane fractions were performed as described (Smeekens et al., 1986). Sucrose step gradient fractionations were performed as described (Li et al., 1991). After gradient separation, the stroma and envelope protein fractions were concentrated by acetone precipitation, whereas the thylakoid membranes were concentrated by centrifugation at 20,000*g* after dilution with 3 volumes of buffer without sucrose. Proteins from import experiments equivalent to 10 μg of chlorophyll were separated by 15% SDS-PAGE, and the gels were fixed in 7% (v/v) acetic acid and 25% (v/v) methanol, stained with Coomassie Brilliant Blue R 250, destained to verify fractionation, and dried. The radiolabeled proteins were visualized using a STORM PhosphorImager (Molecular Dynamics, Sunnyvale, CA). To verify the purity and recovery of sucrose density gradient fractions, proteins were blotted onto nitrocellulose membranes and probed with CpNifS antibody as a stromal marker (Pilon-Smits et al., 2002), with cytochrome *f* antibody as a thylakoid marker (Munekage et al., 2001), or with Tic-110 antibody as an envelope marker (Jackson et al., 1998).

Chlorophyll Fluorescence, Chlorophyll Content, and Metal Ion Measurements

Chlorophyll fluorescence was measured using a MINI-PAM portable chlorophyll fluorometer (Walz, Effeltrich, Germany) as described (Shikanai et al., 2003). Chlorophyll content was determined by absorbance changes in intact leaves as measured with SPAD-502 equipment (Konica Minolta, Tokyo, Japan) (Shikanai et al., 2003). Metal ion content in total leaves, intact chloroplasts, and thylakoid fractions was determined as described (Shikanai et al., 2003). Statistical analysis was performed using the JMP IN software package (SAS Institute, Cary, NC).

Transcript Analysis

Ten micrograms of total RNA was subjected to electrophoresis on a 1% agarose gel containing 4% formaldehyde, transferred to a nylon membrane, and probed with ^{32}P-labeled probes. The probes were obtained by PCR amplification using the following oligonucleotides: for *CSD1*, 5′-GAGTTGCAGTTTTGAACAGC-3′ (sense) and 5′-TTCTTTGGAAACGTAGCAGC-3′ (antisense); for *CSD2*, 5′-AAACGTCAAACATAGCAGCAG-3′ (sense) and 5′-AGTAAACACATCACTGTCAT-3′ (antisense); and for *FeSOD*, 5′-CAAACTCTGGAGTTTCACTG-3′ (sense) and 5′-TCAAGTCTGGCACTTACGC-3′ (antisense). Radioactive probes were synthesized with an oligolabeling kit from Amersham using random primers. Hybridization was performed at 42°C in a solution containing 50% formamide, 5× SSPE (1× SSPE is 0.115 M NaCl, 10 mM sodium phosphate, and 1 mM EDTA, pH 7.4), 5 × Denhardt's solution (1× Denhardt's solution is 0.02% Ficoll, 0.02% polyvinylpyrrolidone, and 0.02% BSA), 0.1% (w/v) SDS, and salmon sperm DNA (100 μg/mL). After hybridization, membranes were washed with 0.1% SSC (1× SSC is 0.15 M NaCl and 0.015 M sodium citrate) and 0.1% SDS at 65°C, and radiolabeled bands were visualized and quantified in a STORM PhosphorImager (Molecular Dynamics).

Because *PAA1* and *PAA2* transcripts were not detectable on RNA gel blots, we used RT-PCR to compare the mRNA abundance of *PAA1* and *PAA2*.Sense (5′-CCGTCTTTCAGGAGTATCTCAAGT-3′) and antisense (5′-AGAGCTTTGCTTCCATCTTGTGTT-3′) primers were used to amplify 2.5 kb of *PAA1*. Sense (5′-TGAATCTTCAATCGAATCTGTGAAAT-3′) and antisense (5′-CAAGCTATTTTTACTTGTTTCAGACT-3′) primers were used to amplify 2.4 kb of *PAA2*. The PCRs were performed in a final volume of 50 μL using serial dilutions of the cDNA as templates. The reaction mixtures were heated at 94°C for 4 min and cooled to 55°C, and 2 units of Ex-Taq polymerase (Takara) was added to initiate the amplification reaction. Thirty-five cycles of amplification were performed in an Eppendorf Mastercycler gradient, each consisting of 1 min of denaturation at 94°C, 1 min of annealing at 55°C, and 2 min of extension at 72°C. The amplified products were resolved by electrophoresis on a 1% agarose gel, blotted onto a nylon membrane, and probed with ^{32}P-labeled gene-specific probes for *PAA1* and *PAA2*. Sense (5′-TAAGCTCTCAAGATCAAAGGCT-3′) and antisense (5′-AACATTGCAAAGAGTTTCAAGGT-3′) primers were used to amplify 200 bp of the actin gene under the same conditions as an internal control.

Analysis of Cu Proteins and Immunoblotting

The relative amounts of apoplastocyanin and holoplastocyanin in thylakoids of the wild type and *PAA2* mutants were analyzed as described (Li et al., 1990; Shikanai et al., 2003). For these experiments, thylakoids were isolated from intact chloroplasts from 4-week-old plants grown on soil. Approximately 100 plants were used for each isolation, and two replicates were performed. Plastocyanin was purified from fresh spinach obtained from a local health food store essentially as described (Yocum, 1982). The purified protein migrated as a single band by SDS-PAGE and was blue with the characteristic absorption spectrum after oxidation with ferricyanide (Yocum, 1982). Apoplastocyanin was produced by treatment with ascorbate and KCN as described by Li et al. (1990). Total shoot protein samples from plants grown on MS-agar plates (~50 seedlings per experiment) for native gel assays were obtained as described (Bowler et al., 1989), and native gel assays for SOD activity were performed as described (Beauchamp and Fridovich, 1971). Three independent replicate assays were performed. The SOD isozymes were identified by differential inhibition using 2 mM KCN to inhibit Cu/ZnSOD (Van Camp et al., 1996) or 3 mM H_2O_2 to inhibit Cu/ZnSOD and FeSOD. For SOD activity in the stroma fractions, intact chloroplasts were isolated from rosette leaves of plants (100 to 200) grown on MS-agar plates as described (Rensink et al., 1998), and stromal protein fractions were obtained as described (Smeekens et al., 1986). Two replicate assays were performed. Antibodies for immunoblot detection of plastocyanin (de Boer et al., 1988), SOD isoforms (Kliebenstein et al., 1998), and CpNifS (Pilon-Smits et al., 2002) have been described. P28 antibodies were a kind gift from S. Bednarek (University of Wisconsin, Madison, WI). Ribulose-1,5-bis-phosphate carboxylase/oxygenase large subunit antibody was purchased from AgriSera (Stockholm, Sweden).

Bound antibodies on blots were detected by the ECF system (Amersham Pharmacia Biotech). Quantification of the bands was performed using ImageQuant software (Molecular Dynamics). Total protein was determined according to Bradford (1976).

Sequence Analyses

Transit sequences and cleavage sites were predicted using the CloroP program at http://www.cbs.dtu.dk/services/ChloroP/ (Emanuelsson et al., 2000). Protein alignments were done using ClustalW (http://www.ebi.ac.uk/clustalw/). The characteristic domains of CPx ATPases indicated by Solioz and Vulpe (1996) were identified in the conserved regions of PAA1 and PAA2. The location of possible transmembrane helices was determined using the program TMHMM at http://www.cbs.dtu.dk/services/TMHMM-2.0/ (Krogh et al., 2001). Hydrophobicity plots were produced according to Kyte and Doolittle (1982) at http://us.expasy.org/tools/protscale.html.

Sequence data from this article have been deposited with the GenBank data library under accession numbers AY297817 for *PAA2* (At5g21930) and BAA23769 for *PAA1* (At4g33520).

ACKNOWLEDGMENTS

We are grateful to Elizabeth Pilon-Smits for critical reading of the manuscript, to Daniel Kliebenstein and Robert Last, Ken Keegstra and John Froehlich, and Sebastian Bednarek for the generous antibody gifts, and to Norbert Rolland for the GFP reporter plasmid. We thank Sabeeha Merchant for helpful discussions. Momoko Miyata is acknowledged for her excellent technical assistance at the Nara Institute of Science and Technology. The BAC clone was obtained from the Arabidopsis Biological Resource Center. This work was supported by grants from the Japanese Society for the Promotion of Science (RFTF96R16004 and J5370024) to T.S., the U.S. Department of Agriculture National Research Initiative (98-35306-6600) and the Searle Scholars Program/The Chicago Community Trust to K.K.N., and the U.S. National Science Foundation (MCB-0091163, DBI-0400706, and IBN-0418993) to M.P.

Received December 20, 2004; accepted February 18, 2005.

REFERENCES

Asada, K. (1999). The water-water cycle in chloroplasts: Scavenging of active oxygen and dissipation of excess photons. Annu. Rev. Plant Physiol. Plant Mol. Biol. **50,** 601–639.

Asakura, Y., Hirohashi, T., Kikuchi, S., Belcher, S., Osborne, E., Yano, S., Terashima, I., Barkan, A., and Nakai, M. (2004). Maize mutants lacking chloroplast FtsY exhibit pleiotropic defects in the biogenesis of thylakoid membranes. Plant Cell **16,** 201–214.

Askwith, C., Eide, D., Van Ho, A., Bernard, P.S., Li, L., Davis-Kaplan, S., Sipe, D.M., and Kaplan, J. (1994). The FET3 gene of *S. cerevisiae* encodes a multicopper oxidase required for ferrous iron uptake. Cell **76,** 403–410.

Axelsen, K.B., and Palmgren, M.G. (2001). Inventory of the superfamily of P-type ion pumps in Arabidopsis. Plant Physiol. **126,** 696–706.

Baxter, I., Tchieu, J., Sussman, M.R., Boutry, M., Palmgren, M.G., Gribskov, M., Harper, J.F., and Axelsen, K.B. (2003). Genomic comparison of P-type ATPase ion pumps in Arabidopsis and rice. Plant Physiol. **132,** 618–628.

Beauchamp, C., and Fridovich, I. (1971). Superoxide dismutase: Improved assays and an assay applicable to acrylamide gels. Anal. Biochem. **44,** 276–287.

Bowler, C., Alliotte, T., De Loose, M., Van Montagu, M., and Inzé, D. (1989). The induction of manganese superoxide dismutase in response to stress in *Nicotiana plumbaginifolia*. EMBO J. **8,** 31–38.

Bowler, C., Van Camp, W., Van Montagu, M., and Inzé, D. (1994). Superoxide dismutase in plants. Crit. Rev. Plant Sci. **13,** 199–218.

Bowler, C., Van Montagu, M., and Inzé, D. (1992). Superoxide dismutase and stress tolerance. Annu. Rev. Plant Physiol. Plant Mol. Biol. **43,** 83–116.

Bradford, M.M. (1976). A rapid and sensitive method for the quantitation of microgram quantities of protein utilizing the principle of protein-dye binding. Anal. Biochem. **72,** 248–254.

Brown, J.W., Smith, P., and Simpson, C. (1996). *Arabidopsis* consensus intron sequences. Plant Mol. Biol. **32,** 531–535.

Clough, S.J., and Bent, A.F. (1998). Floral dip: A simplified method for Agrobacterium-mediated transformation of *Arabidopsis thaliana*. Plant J. **16,** 735–743.

Culotta, V.C., Joh, H.D., Lin, S.J., Slekar, K.H., and Strain, J. (1995). A physiological role for *Saccharomyces cerevisiae* copper/zinc superoxide dismutase in copper buffering. J. Biol. Chem. **270,** 29991–29997.

Dancis, A., Yuan, D.S., Haile, D., Askwith, C., Eide, D., Moehle, C., Kaplan, J., and Klausner, R.D. (1994). Molecular characterization of a copper transport protein in *S. cerevisiae*: An unexpected role for copper in iron transport. Cell **76,** 393–402.

de Boer, D., Cremers, R., Teertstra, L., Smits, L., Smeekens, S., and Weisbeek, P. (1988). In vivo import of plastocyanin and a fusion protein in developmentally different plastids of transgenic plants. EMBO J. **7,** 2631–2635.

Emanuelsson, O., Nielsen, H., Brunak, S., and von Heijne, G. (2000). Predicting subcellular localization of proteins based on their N-terminal amino acid sequence. J. Mol. Biol. **300,** 1005–1016.

Escoubas, J.M., Lomas, M., LaRoche, J., and Folkowski, P.G. (1995). Light intensity regulation of cab gene transcription is signaled by the redox state of the plastoquinone pool. Proc. Natl. Acad. Sci. USA **92,** 10237–10241.

Fox, T.C., and Guerinot, M.L. (1998). Molecular biology of cation transport in plants. Annu. Rev. Plant Physiol. Plant Mol. Biol. **49,** 669–696.

Friso, G., Giacomelli, L., Ytterberg, A.J., Peltier, J.-P., Rudella, A., Sun, Q., and Van Wijk, K.J. (2004). In-depth analysis of the thylakoid membrane proteome of *Arabidopsis thaliana* chloroplasts: New proteins, new functions, and a plastid proteome database. Plant Cell **16,** 478–499.

Genty, B., Briantais, J.-M., and Baker, N.R. (1989). The relationship between quantum yield of photosynthetic electron transport and quenching of chlorophyll fluorescence. Biochim. Biophys. Acta **990,** 87–92.

Gravot, A., Lieutaud, A., Verret, F., Auroy, P., Vavasseur, A., and Richaud, P. (2004). AtHMA3, a plant P1B-ATPase, functions as a Cd/Pb transporter in yeast. FEBS Lett. **561,** 22–28.

Guo, W.-J., Bundithya, W., and Goldsbrough, P.B. (2003). Characterization of the *Arabidopsis* metallothionein gene family: Tissue specific expression and induction during senescence and in response to copper. New Phytol. **159,** 369–381.

Himelblau, E., and Amasino, R.M. (2000). Delivering copper within plant cells. Curr. Opin. Plant Biol. **3,** 205–210.

Himelblau, E., Mira, H., Lin, S.J., Culotta, V.C., Penarrubia, L., and Amasino, R.M. (1998). Identification of a functional homolog of the yeast copper homeostasis gene ATX1 from Arabidopsis. Plant Physiol. **117,** 1227–1234.

Hirayama, T., Kieber, J.J., Hirayama, N., Kogan, M., Guzman, P., Nourizadeh, S., Alonso, J.M., Dailey, W.P., Dancis, A., and Ecker, J.R. (1999). RESPONSIVE-TO-ANTAGONIST1, a Menkes/Wilson disease-related copper transporter, is required for ethylene signaling in *Arabidopsis*. Cell **97,** 383–393.

Hussain, D., Haydon, M.J., Wang, Y., Wong, E., Sherson, S.M., Young, J., Camakaris, J., Harper, J.F., and Cobbett, C.S. (2004). P-type ATPase heavy metal transporters with roles in essential zinc homeostasis in Arabidopsis. Plant Cell **16,** 1327–1339.

Inoue, K., and Keegstra, K. (2003). A polyglycine stretch is necessary for proper targeting of the protein translocation channel precursor to the outer envelope membrane of chloroplasts. Plant J. **34,** 661–669.

Jackson, D., Froehlich, J., and Keegstra, K. (1998). The hydrophilic domain of Tic110, an inner envelope membrane component of the chloroplastic protein translocation apparatus, faces the stromal compartment. J. Biol. Chem. **273,** 16583–16588.

Kampfenkel, K., Kushnir, S., Babiychuk, E., Inze, D., and Van Montagu, M. (1995). Molecular characterization of a putative *Arabidopsis thaliana* copper transporter and its yeast homologue. J. Biol. Chem. **270,** 28479–28486.

Kanamaru, K., Kashiwagi, S., and Mizuno, T. (1994). A copper-transporting P-type ATPase found in the thylakoid membrane of the cyanobacterium *Synechococcus* species PCC7942. Mol. Microbiol. **13,** 369–377.

Keegstra, K., and Froehlich, J.E. (1999). Protein import into chloroplasts. Curr. Opin. Plant Biol. **2,** 471–476.

Kliebenstein, D.J., Monde, R.A., and Last, R.L. (1998). Superoxide dismutase in Arabidopsis: An eclectic enzyme family with disparate regulation and protein localization. Plant Physiol. **118,** 637–650.

Konieczny, A., and Ausubel, F.M. (1993). A procedure for mapping *Arabidopsis* mutations using co-dominant ecotype-specific PCR-based markers. Plant J. **4,** 403–410.

Krause, G.H., and Weis, E. (1991). Chlorophyll fluorescence and photosynthesis: The basics. Annu. Rev. Plant Physiol. Plant Mol. Biol. **42,** 313–349.

Krogh, A., Larsson, B., von Heijne, G., and Sonnhammer, E.L.L. (2001). Predicting transmembrane protein topology with a hidden Markov model: Application to complete genomes. J. Mol. Biol. **305,** 567–580.

Kyte, J., and Doolittle, R.F. (1982). A simple method for displaying the hydropathic character of a protein. J. Mol. Biol. **157,** 105–132.

La Fontaine, S., Quinn, J.M., Nakamoto, S.S., Page, M.D., Gohre, V., Moseley, J.L., Kropat, J., and Merchant, S. (2002). Copper-dependent iron assimilation pathway in the model photosynthetic eukaryote *Chlamydomonas reinhardtii*. Eukaryot. Cell **1,** 736–757.

Li, H.H., and Merchant, S. (1995). Degradation of plastocyanin in copper-deficient *Chlamydomonas reinhardtii*: Evidence for a protease-susceptible conformation of the apoprotein and regulated proteolysis. J. Biol. Chem. **270,** 23504–23510.

Li, H.M., Moore, H., and Keegstra, K. (1991). Targeting of proteins to the outer envelope membrane uses a different pathway than transport into chloroplast. Plant Cell **3,** 709–717.

Li, H.M., Theg, S.M., Bauerle, C.M., and Keegstra, K. (1990). Metal-ion-center assembly of ferredoxin and plastocyanin in isolated chloroplasts. Proc. Natl. Acad. Sci. USA **87,** 6748–6752.

Lin, S.J., Pufahl, R.A., Dancis, A., O'Halloran, T.V., and Culotta, V.C. (1997). A role for the *Saccharomyces cerevisiae* ATX1 gene in copper trafficking and iron transport. J. Biol. Chem. **272,** 9215–9220.

Marschner, H. (1995). Mineral Nutrition of Higher Plants. (London: Academic Press).

Mills, R.F., Krijger, G.C., Baccarini, P.J., Hall, J.L., and Williams, L.E. (2003). Functional expression of AtHMA4, a P1B-type ATPase of the Zn/Co/Cd/Pb subclass. Plant J. **35,** 164–176.

Molina-Heredia, F.P., Wastl, J., Navarro, J.A., Bendall, D.S., Hervas, M., Howe, C.J., and De La Rosa, M.A. (2003). Photosynthesis: A new function for an old cytochrome? Nature **424,** 33–34.

Munekage, Y., Takeda, S., Endo, T., Jahns, P., Hashimoto, T., and Shikanai, T. (2001). Cytochrome b_6f mutation specifically affects thermal dissipation of absorbed light energy in *Arabidopsis*. Plant J. **28,** 351–359.

Murphy, A., and Taiz, L. (1995). A new vertical mesh transfer technique for metal-tolerance studies in Arabidopsis (ecotypic variation and copper-sensitive mutants). Plant Physiol. **108,** 29–38.

Nelson, N. (1999). Metal ion transporters and homeostasis. EMBO J. **18,** 4361–4371.

Niyogi, K.K., Grossman, A.R., and Björkman, O. (1998). Arabidopsis mutants define a central role for the xanthophyll cycle in the regulation of photosynthetic energy conversion. Plant Cell **10,** 1121–1134.

Outten, F.W., Huffman, D.L., Hale, J.A., and O'Halloran, T.V. (2001). The independent cue and cus systems confer copper tolerance during aerobic and anaerobic growth in *Escherichia coli*. J. Biol. Chem. **276,** 30670–30677.

Peltier, J.B., Emanuelsson, O., Kalume, D.E., Ytterberg, J., Friso, G., Rudella, A., Liberles, D.A., Soderberg, L., Roepstorff, P., von Heijne, G., and van Wijk, K.J. (2002). Central functions of the lumenal and peripheral thylakoid proteome of Arabidopsis determined by experimentation and genome-wide prediction. Plant Cell **14,** 211–236.

Petrovic, N., Comi, A., and Ettinger, M.J. (1996). Identification of an apo-superoxide dismutase (Cu,Zn) pool in human lymphoblasts. J. Biol. Chem. **271,** 28331–28334.

Phung, L.T., Ajlani, G., and Haselkorn, R. (1994). P-type ATPase from the cyanobacterium *Synechococcus* 7942 related to the human Menkes and Wilson disease gene products. Proc. Natl. Acad. Sci. USA **91,** 9651–9654.

Pilon, M., de Kruijff, B., and Weisbeek, P.J. (1992). New insights into

the import mechanism of the ferredoxin precursor into chloroplasts. J. Biol. Chem. **267,** 2548–2556.

Pilon-Smits, E.A., Garifullina, G.F., Abdel-Ghany, S., Kato, S., Mihara, H., Hale, K.L., Burkhead, J.L., Esaki, N., Kurihara, T., and Pilon, M. (2002). Characterization of a NifS-like chloroplast protein from Arabidopsis: Implications for its role in sulfur and selenium metabolism. Plant Physiol. **130,** 1309–1318.

Pufahl, R.A., Singer, C.P., Peariso, K.L., Lin, S.J., Schmidt, P.J., Fahrni, C.J., Culotta, V.C., Penner-Hahn, J.E., and O'Halloran, T.V. (1997). Metal ion chaperone function of the soluble Cu(I) receptor Atx1. Science **278,** 853–856.

Rae, T.D., Schmidt, P.J., Pufahl, R.A., Culotta, V.C., and O'Halloran, T.V. (1999). Undetectable intracellular free copper: The requirement of a copper chaperone for superoxide dismutase. Science **284,** 805–808.

Raven, J.A., Evans, M.C., and Korb, R.E. (1999). The role of trace metals in photosynthetic electron transport in O_2-evolving organisms. Photosynth. Res. **60,** 111–149.

Rensing, C., and Grass, G. (2003). *Escherichia coli* mechanisms of copper homeostasis in a changing environment. FEMS Microbiol. Rev. **27,** 197–213.

Rensing, C., Fan, B., Sharma, R., Mitra, B., and Rosen, B.P. (2000). CopA: An *Escherichia coli* Cu(I)-translocating P-type ATPase. Proc. Natl. Acad. Sci. USA **97,** 652–656.

Rensink, W.A., Pilon, M., and Weisbeek, P. (1998). Domains of a transit sequence required for in vivo import in Arabidopsis chloroplasts. Plant Physiol. **118,** 691–699.

Rizhsky, L., Liang, H., and Mittler, R. (2003). The water-water cycle is essential for chloroplast protection in the absence of stress. J. Biol. Chem. **278,** 38921–38925.

Sancenon, V., Puig, S., Mira, H., Thiele, D.J., and Penarrubia, L. (2003). Identification of a copper transporter family in *Arabidopsis thaliana*. Plant Mol. Biol. **51,** 577–587.

Schnell, D.J. (1998). Protein targeting in the thylakoid membrane. Annu. Rev. Plant Physiol. Plant Mol. Biol. **49,** 97–126.

Schubert, M., Petersson, U.A., Haas, B.J., Funk, C., Schroder, W.P., and Kieselbach, T. (2002). Proteome map of the chloroplast lumen of *Arabidopsis thaliana*. J. Biol. Chem. **277,** 8354–8365.

Shikanai, T., Müller-Moulé, P., Munekage, Y., Niyogi, K.K., and Pilon, M. (2003). PAA1, a P-type ATPase of Arabidopsis, functions in copper transport in chloroplasts. Plant Cell **15,** 1333–1346.

Shikanai, T., Munekage, Y., Shimizu, K., Endo, T., and Hashimoto, T. (1999). Identification and characterization of *Arabidopsis* mutants with reduced quenching of chlorophyll fluorescence. Plant Cell Physiol. **40,** 1134–1142.

Shingles, R., Wimmers, L.E., and McCarthy, R.E. (2004). Copper transport across pea thylakoid membranes. Plant Physiol. **135,** 145–151.

Smeekens, S., Bauerle, C., Hageman, J., Keegstra, K., and Weisbeek, P. (1986). The role of the transit peptide in the routing of precursors toward different chloroplast compartments. Cell **46,** 365–375.

Solioz, M., and Vulpe, C. (1996). CPx-type ATPases: A class of P-type ATPases that pump heavy metals. Trends Biochem. Sci. **21,** 237–241.

Tabata, K., Kashiwagi, S., Mori, H., Ueguchi, C., and Mizuno, T. (1997). Cloning of a cDNA encoding a putative metal-transporting P-type ATPase from *Arabidopsis thaliana*. Biochim. Biophys. Acta **1326,** 1–6.

Tottey, S., Rich, P.R., Rondet, S.A., and Robinson, N.J. (2001). Two Menkes-type ATPases supply copper for photosynthesis in *Synechocystis* PCC 6803. J. Biol. Chem. **276,** 19999–20004.

Tottey, S., Rondet, S.A., Borrelly, G.P., Robinson, P.J., Rich, P.R., and Robinson, N.J. (2002). A copper metallochaperone for photosynthesis and respiration reveals metal-specific targets, interaction with an importer, and alternative sites for copper acquisition. J. Biol. Chem. **277,** 5490–5497.

Tsang, E.W., Bowler, C., Herouart, D., Van Camp, W., Villarroel, R., Genetello, C., Van Montagu, M., and Inze, D. (1991). Differential regulation of superoxide dismutases in plants exposed to environmental stress. Plant Cell **3,** 783–792.

Van Camp, W., Capiau, K., Van Montagu, M., Inze, D., and Slooten, L. (1996). Enhancement of oxidative stress tolerance in transgenic tobacco plants overproducing Fe-superoxide dismutase in chloroplasts. Plant Physiol. **112,** 1703–1714.

Weigel, M., Varotto, C., Pesaresi, P., Finazzi, G., Rappaport, F., Salamini, F., and Leister, D. (2003). Plastocyanin is indispensable for photosynthetic electron flow in *Arabidopsis thaliana*. J. Biol. Chem. **278,** 31286–31289.

Williams, L.E., Pittman, J.K., and Hall, J.L. (2000). Emerging mechanisms for heavy metal transport in plants. Biochim. Biophys. Acta **1465,** 104–126.

Woeste, K.E., and Kieber, J.J. (2000). A strong loss-of-function mutation in RAN1 results in constitutive activation of the ethylene response pathway as well as a rosette-lethal phenotype. Plant Cell **12,** 443–455.

Yocum, C.F. (1982). Purification of ferredoxin and plastocyanin. In Methods in Chloroplast Molecular Biology, M. Edelman, R.B. Hallick, and N.-H. Chua, eds (Amsterdam: Elsevier Biomedical Press), pp. 973–981.

Yuan, D.S., Stearman, R., Dancis, A., Dunn, T., Beeler, T., and Klausner, R.D. (1995). The Menkes/Wilson disease gene homologue in yeast provides copper to a ceruloplasmin-like oxidase required for iron uptake. Proc. Natl. Acad. Sci. USA **92,** 2632–2636.